PNNL-14700

Pacific Northwest
National Laboratory
Operated by Battelle for the
U.S. Department of Energy

Near-Field Hydrology Data Package For the Integrated Disposal Facility 2005 Performance Assessment

P. D. Meyer
K. P. Saripalli
V. L. Freedman

June 2004

Prepared for the U.S. Department of Energy
under Contract DE-AC06-76RL01830

DISCLAIMER

PACIFIC NORTHWEST NATIONAL LABORATORY
operated by
BATTELLE
for the

UNITED STATES DEPARTMENT OF ENERGY

under Contract DE-AC06-76RL01830

Printed in the United States of America

Available to DOE and DOE contractors from the
Office of Scientific and Technical Information,
P.O. Box 62, Oak Ridge, TN 37831-0062;
ph: (865) 576-8401
fax: (865) 576-5728
email: reports@adonis.osti.gov

Available to the public from the National Technical Information Service,
U.S. Department of Commerce, 5285 Port Royal Rd., Springfield, VA 22161
ph: (800) 553-6847
fax: (703) 605-6900
email: orders@ntis.fedworld.gov
online ordering: http://www.ntis.gov/ordering.htm

PNNL-14700

Near-Field Hydrology Data Package for the Integrated Disposal Facility 2005 Performance Assessment

P. D. Meyer
K. P. Saripalli
V. L. Freedman

June 2004

Prepared for
the U.S. Department of Energy
under Contract DE-AC06-76RL01830

Pacific Northwest National Laboratory
Richland, Washington 99352

Summary

CH2MHill Hanford Group, Inc. (CHG) is designing and assessing the performance of an Integrated Disposal Facility (IDF) to receive Immobilized Low-Activity Waste (ILAW), Low-Level and Mixed Low-Level Wastes (LLW/MLLW), and the Waste Treatment Plant (WTP) melters used to vitrify the ILAW. The IDF Performance Assessment (PA) assesses the performance of the disposal facility to provide a reasonable expectation that the disposal of the waste is protective of the general public, groundwater resources, air resources, surface water resources, and inadvertent intruders. The PA requires prediction of contaminant migration from the facilities, which is expected to occur primarily via the movement of water through the facilities and the consequent transport of dissolved contaminants in the vadose zone and groundwater.

Pacific Northwest National Laboratory (PNNL) assists CHG in its performance assessment activities. One of PNNL's tasks is to provide estimates of the physical, hydraulic, and transport properties of the materials comprising the disposal facilities and the disturbed region around them. These materials are referred to as the near-field materials. Their properties are expressed as parameters of constitutive models used in simulations of subsurface flow and transport. In addition to the best-estimate parameter values, information on uncertainty in the parameter values and estimates of the changes in parameter values over time are required to complete the PA. These parameter estimates and information were previously presented in a report prepared for the 2001 ILAW PA. That PA assumed that the disposal facility would contain only ILAW and that the waste packages would be disposed of in a buried concrete vault. In addition to changes in the facility design and waste characteristics, additional information and data have been collected to better define some of the material properties. This report provides near-field material parameter estimates for the 2005 IDF PA using applicable information from the previous report, revised to reflect changes in the facility and to include the latest available data and information on parameter values.

Acknowledgments

Technical review of this report was provided by Gene Freeman, Pacific Northwest National Laboratory. His detailed comments contributed to the technical soundness and readability of the report. We also appreciate the comments provided by Fred Mann and Jim Field of CH2MHill Hanford Group, Inc.

Contents

Figures

Tables

1.0 Introduction

The Hanford Site was established in 1944 as a U.S. Government nuclear materials production facility. During its history, site missions included nuclear reactor operation, storage and reprocessing of spent nuclear fuel, and management of radioactive and hazardous wastes. Today, activities on the site involve environmental restoration, energy-related research, and technology development. Over fifty years of operations have resulted in the accumulation of significant quantities of radioactive and hazardous wastes as well as their release to the environment. Figure 1.1 shows the location of the Hanford Site within Washington State, the boundaries of the Hanford Site, and the location of the major facilities. The 100 Areas are the sites of reactor facilities. The major processing facilities, waste storage facilities, and waste disposal areas are located in the 200 Areas.

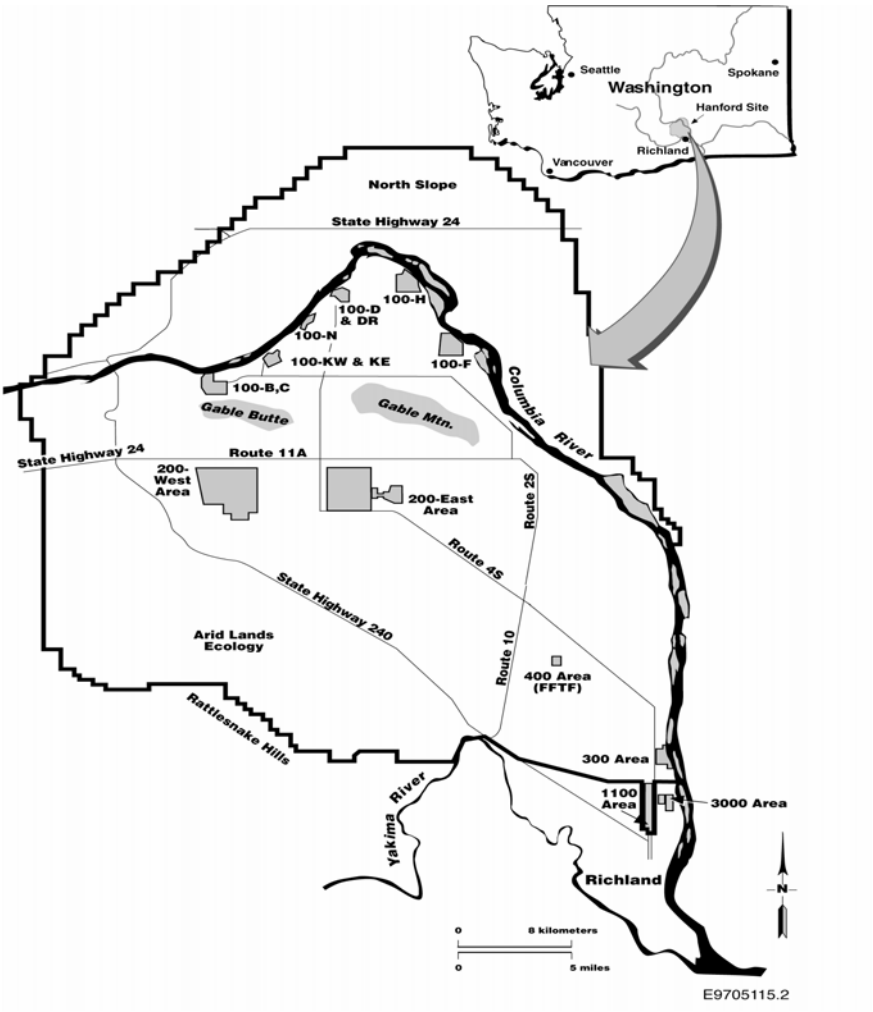

Figure 1.1. The Hanford Site and its Location within Washington State

1.1 Integrated Disposal Facility

As part of its environmental restoration mission, the U.S. Department of Energy (DOE) is proceeding with plans to permanently dispose of a variety of wastes on the Hanford Site. As part of the Hanford Site Solid Waste Program Environmental Impact Statement (DOE 2004), DOE identified its preferred alternative for onsite disposal of solid (radioactive and hazardous) wastes. The preferred alternative involves disposal in a new facility located in the south-central part of the 200 East Area, referred to as the Integrated Disposal Facility (IDF). Figure 1.2 illustrates the location of the IDF.

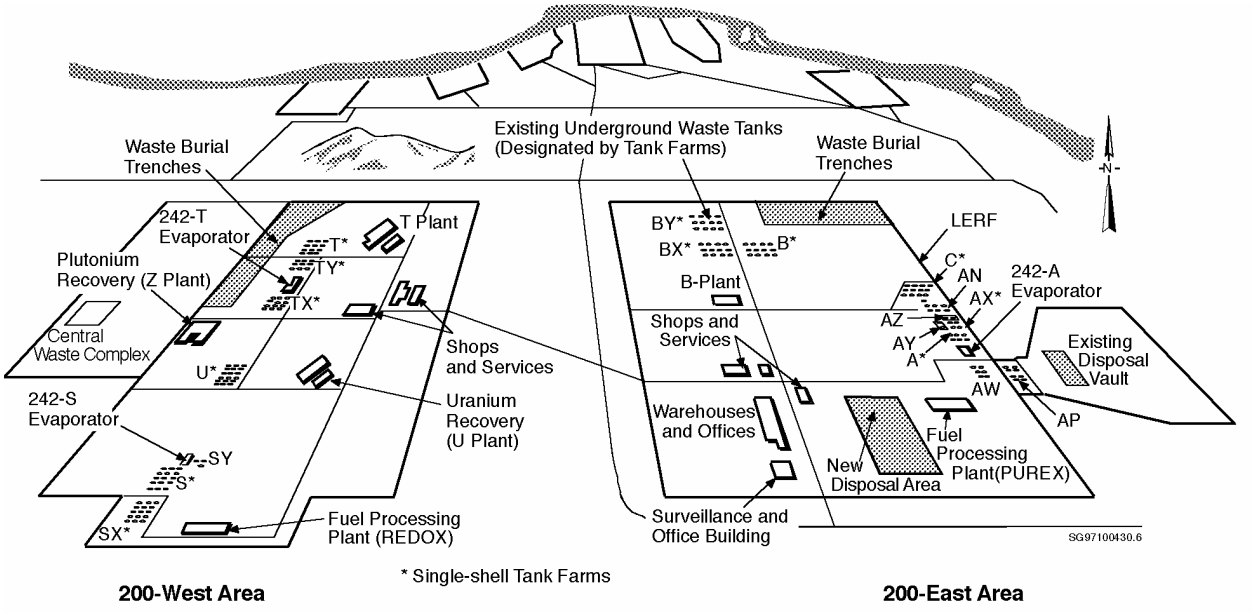

Figure 1.2. Hanford 200 Areas. The Integrated Disposal Facility is located in the south-central part of the 200 East Area and is labeled "New Disposal Area."

Several categories of waste are planned to be disposed in the IDF. These categories are:

- Immobilized Low-Activity Waste (ILAW) – This is Hanford tank waste that has undergone separations treatment to remove the bulk of the radionuclides as a high level waste stream. The remaining low-activity waste stream will be solidified at the Hanford Waste Treatment and Immobilization Plant (WTP) using a vitrification process. Alternative processes to immobilize the low-activity waste (supplemental to the baseline vitrification process) are being considered (CHG 2003a; Mann et al. 2003b).

- Failed or decommissioned WTP melters.

- Low-Level Waste (LLW) – This is waste that contains man-made radionuclides, but which is not classified as high-level waste or transuranic waste. Some LLW disposed of at the IDF may originate off-site.

- Mixed Low-Level Waste (MLLW) – This is LLW waste that also contains hazardous materials regulated under the Resource Conservation and Recovery Act (RCRA) or the corresponding dangerous waste management laws of the State of Washington.

The IDF is to be constructed as a double-lined trench with two initial disposal cells and room for future expansion of the cells. A protective surface cover will be constructed over the trench prior to closure. Additional details on disposal facility design are given in Section 2.2 and in Puigh (2004).

1.2 IDF Performance Assessment

Radiological performance objectives and dangerous material (hazardous chemical) performance goals proposed for use in the 2005 IDF PA are described in Mann (2002). The radiological performance objectives include dose limits for an all-pathways scenario and an inadvertent intruder scenario as well as concentration and dose limits in groundwater, surface water, and air. Performance objectives are evaluated for 1,000 years (except for the inadvertent intruder scenario), but are calculated to the time of peak or 10,000 years, whichever is longer. In addition to a base case simulation, sensitivity calculations will be performed to demonstrate that the design for the IDF disposal achieves impacts that are as low as reasonably achievable (ALARA).

The current PA for the IDF facility is the *Hanford Immobilized Low-Activity Waste Performance Assessment: 2001 Version* (Mann et al. 2001). The ILAW PA is updated annually, most recently as Mann (2003). The 2001 ILAW PA was prepared assuming that only ILAW would be disposed at the IDF location. The most recent annual summary acknowledges the anticipated changes in the waste types to be disposed at the facility. A risk assessment for the IDF was recently prepared that considers the combined disposal of ILAW, LLW, MLLW, and the WTP melters in a single facility (Mann et al. 2003a). This risk assessment uses information from the ILAW PA (Mann et al. 2001) and the PA's completed for the Hanford Solid Waste Burial Grounds (Wood et al. 1995; Wood et al. 1996).

Previous long-term environmental assessments at the Hanford Site have consistently shown that the groundwater pathway is the most important (Mann et al. 2003a). This pathway involves water movement into and through the disposal facility, dissolution of the waste, transport of contaminants out of the facility and through the vadose zone to the unconfined aquifer, transport in the aquifer to an extraction well, and human exposure via domestic use of the pumped water. To support the IDF PA a variety of data have been collected and analyses performed to document the geologic, geochemical, and hydraulic conditions at the IDF site, the expected recharge during the life of the facility, the hydraulic and transport conditions within the facility, and the waste form release (for ILAW). These data and analyses were documented in a set of data packages published prior to the 2001 ILAW PA (Mann and Puigh 2001) and included in the PA as appendices. In preparation for a revision of the 2001 ILAW PA (the 2005 IDF PA), these data packages are being updated with additional data and analyses conducted in the intervening years. These additional data packages include information on geology (Reidel 2004), recharge (Fayer and

Szecsody 2004), flow and transport in the natural sediments (Khaleel 2004), geochemistry (Krupka et al. 2004), and waste form release (Pierce et al. 2004).

The near-field hydrology data package for the 2001 ILAW PA (Meyer and Serne 1999) provided estimates of the physical, hydraulic, and transport properties of the materials comprising the ILAW disposal facilities and the disturbed region around them. These materials are referred to as the near-field materials. Their properties are expressed as parameters of constitutive models used in simulations of subsurface flow and transport. In addition to the best-estimate parameter values (used in the base case PA simulation), information on uncertainty in the parameter values and estimates of the changes in parameter values over time were provided for use in sensitivity simulations. Additional data collection and analyses have been conducted since the publication of the near-field hydrology data package. This report revises parameter estimates and related information for the near-field materials associated with the 2005 IDF PA.

The report is organized as follows. Chapter 2 describes the IDF facility design and the near-field materials, including any specifications. Chapter 3 is a definition of the physical, hydraulic, and transport parameters for which values are provided in this report. Chapters 4 and 5 provide the best-estimate hydraulic and transport parameters for the near-field materials. Chapter 6 examines several factors affecting parameter values and Chapter 7 contains concluding remarks.

2.0 Facility Design and Description of Near-Field Materials

A brief summary of the hydrologic and geologic setting of the IDF disposal facility is presented in this section. This is followed by a discussion of the current design of the disposal facility and the near-field materials to be used in its construction.

2.1 Hydrologic and Geologic Setting

The Hanford Site is located in the semiarid Pasco Basin of the Columbia Plateau in southeastern Washington State, within the rain shadow of the Cascade Mountain Range. The Hanford Meteorological Station, located between the 200 East and 200 West Areas on the Hanford Site, has been collecting climatological data representative of the IDF disposal site since 1945 (Hoitink et al. 2003). Precipitation at the Hanford Meteorological Station has averaged 17.2 cm/yr. since 1946, with 52 percent of the annual precipitation occurring from November through February. Days with more than 1.3 cm of precipitation occur on average less than once each year. Rainfall intensities of 1.3 cm/hr. with a duration of one hour are expected to occur once every 10 years. Rainfall intensities of 2.5 cm/hr. with a one-hour duration are expected to occur once every 500 years. Monthly average snowfall ranges from 0.8 cm in March to 13.7 cm in December. The maximum recorded monthly snowfall is 60 cm; the maximum recorded seasonal snowfall is 142 cm. On average, snowfall accounts for about 38% of precipitation from December through February.

Average daily maximum temperature varies from 2ºC in late December and early January to 35ºC in late July. On average, there are 52 days during the summer months with a maximum temperature greater than or equal to 32ºC and 12 days with a maximum temperature greater than 38ºC. From mid-November through early March, minimum temperatures average less than or equal to 0ºC. The recorded maximum temperature is 45ºC; the recorded minimum is -31ºC.

The Hanford Site is characterized as a shrub-steppe ecosystem that is adapted to the region's mid-latitude, semiarid climate (Neitzel 1998). Such ecosystems are typically dominated by a shrub overstory with a grass understory. Livestock grazing and agricultural production prior to government control of the Hanford Site contributed to colonization by non-native vegetation species that currently dominate portions of the landscape. In addition, summer range fires have tended to eliminate fire-intolerant species and have allowed more opportunistic and fire-resistant species a chance to become established. The dominant non-native species on the site is cheatgrass.

Three soil types occur in the vicinity of the IDF disposal sites. As described by Hajek (1966), these soils are: Burbank Loamy Sand, a coarse-textured soil usually about 40 cm thick, underlain by a subsoil with a gravel content ranging from 20 to 80 volume percent; Ephrata Sandy Loam, a medium-textured soil underlain by gravelly material; and Rupert Sand, generally characterized as a coarse sand developed under grass, sagebrush, and hopsage in coarse sandy alluvial deposits.

The semiarid climate results in fairly low rates of groundwater recharge. Natural recharge rates across the Hanford Site are estimated to range from 0 to more than 10 cm/yr depending on surface soils, vegetation, and topography (Fayer and Walters 1995). Minimal recharge rates occur in fine-textured soils

where deep-rooted plants prevail. Larger recharge rates are likely to occur in areas with coarse, gravelly surface sediments and little or no vegetation. Estimates of the recharge rates expected to occur on the IDF disposal site are provided in Fayer and Szecsody (2004).

The IDF disposal site is located on the Cold Creek bar (commonly referred to as the 200 Areas Plateau), a geomorphic remnant of the cataclysmic floods of the Pleistocene epoch (the Missoula Floods). The stratigraphy in the area consists of basalt flows overlain by the Ringold Formation sediments, Hanford Formation sediments, and surficial deposits. The Ringold Formation consists of clay, silt, compacted mud, fine- to coarse-grained sand and granular to cobble gravel. The Hanford Formation, deposited by the Missoula Floods, consists of pebble-to-boulder sized gravel, fine- to coarse-grained sand, and silt. The fine-grained sediments were deposited under slackwater and backflooded conditions. The surficial sediments consist of alluvial and eolian silt, sand, and gravel deposits that are generally less than 5 m thick. The southernmost 200 m of the IDF disposal site is covered with a stabilized sand dune that is as much as 8-m high (see Figure 2.4). Reidel (2004) provides detailed information on the available geologic information for the IDF disposal site based on data from a number of boreholes and wells in the area of the IDF (see Figure 2.1).

The IDF disposal facility will be constructed in excavations within the surficial and upper Hanford Formation sediments. Excavations are likely to be no more than 15-m deep. Reidel (2004) describes the upper portion of the Hanford formation as a sand-dominated facies consisting of fine to coarse-grained sand with minor amounts of silt and clay and some gravelly sands. Reidel (2004) states that the texture of the sand-dominated facies changes across the IDF Site (see Figure 2.2) with increasing sand content, and decreasing silt/clay content, towards the east. Northeast of the site (Borehole 299-E24-4) gravel content increases at the expense of the sand content. These effects occur mainly at a depth greater than 15 m (50 ft.). The upper 15 m consists primarily of sand sediments with a significant gravel content observed over a small fraction of the depth in each borehole.

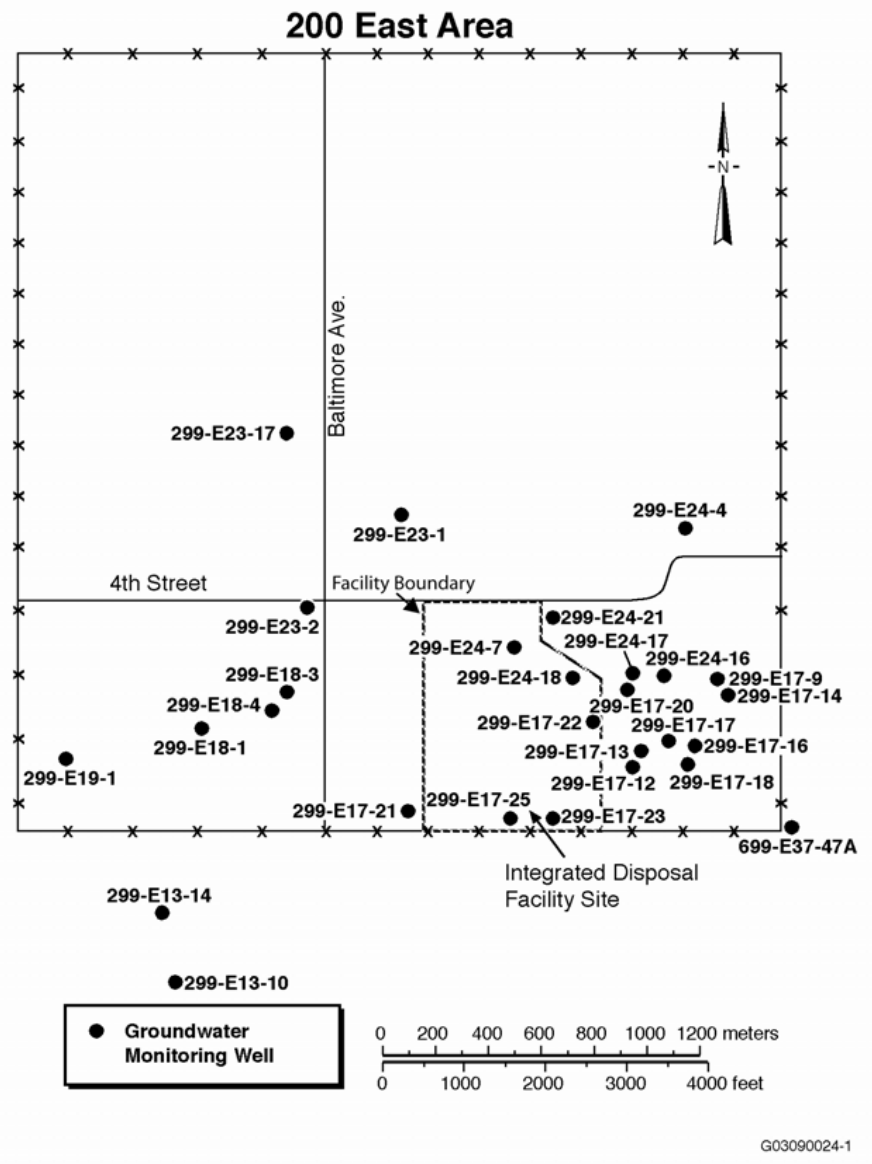

Figure 2.1. Location of Wells Used in Reidel (2004) to Interpret the IDF Site Geology

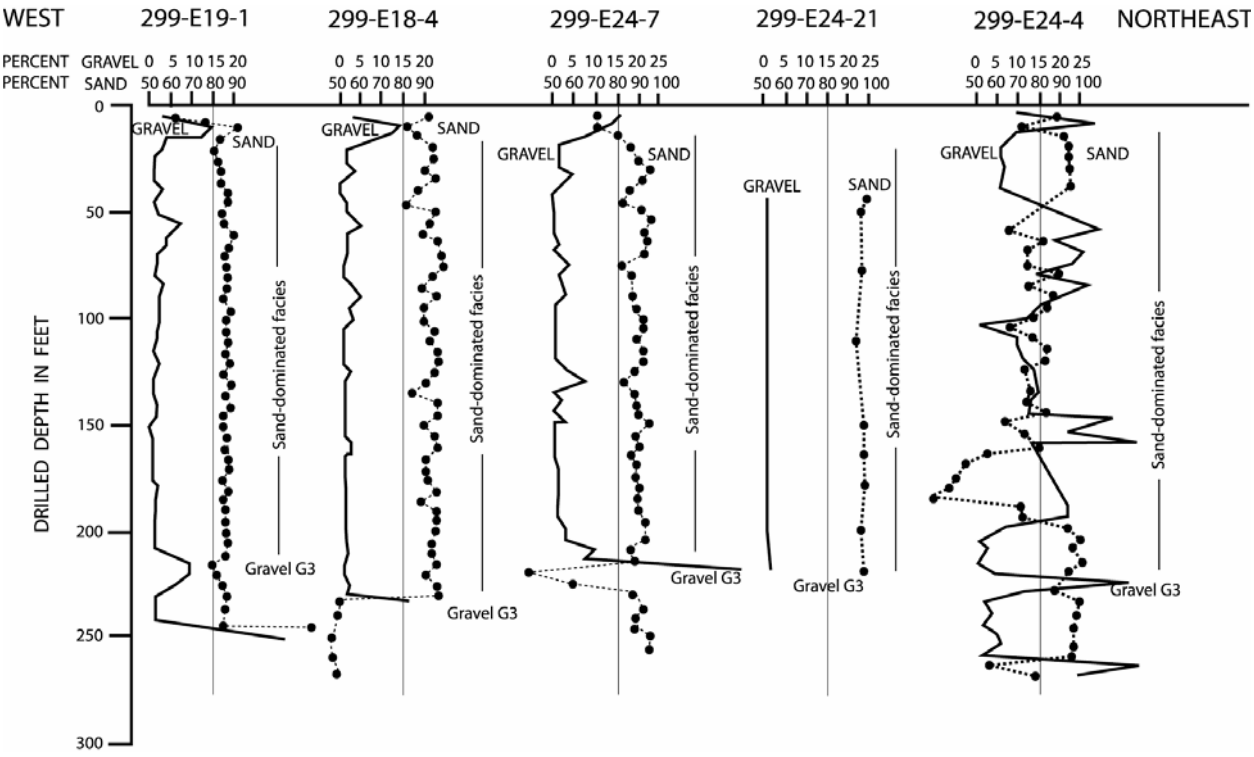

Figure 2.2. Percentage of Sand and Gravel Present in the Upper Part of the Sand-Dominated Facies of the Hanford Formation Near the IDF Site (from Reidel 2004). For comparison, a reference line is drawn at 80% sand, 15% gravel.

2.2 Facility Design

The IDF is to be constructed as a double-lined trench with two initial disposal cells and room for expansion of the cells as shown in Figure 2.3 (CHG 2003b, 2003c). Figure 2.4 and Figure 2.5 are cross-sections through the trench illustrating the trench geometry. Figure 2.6 provides details of the trench liner system, which relies on two geomembrane liners for control of moisture. Prior to closure, a protective surface cover will be constructed over the trench to provide a barrier to vertical water flow (Burbank 2002). Components of the cover will also serve as an inadvertent intruder barrier. It is anticipated that the surface cover will consist of a Modified RCRA Subtitle C Barrier Design as described in DOE (1993a). The components of this cover and their minimum thicknesses are shown in Figure 2.7. The combined minimum thickness of the cover is 1.7 m. Puigh (2004) provides a discussion of the IDF facility design as it relates to the PA.

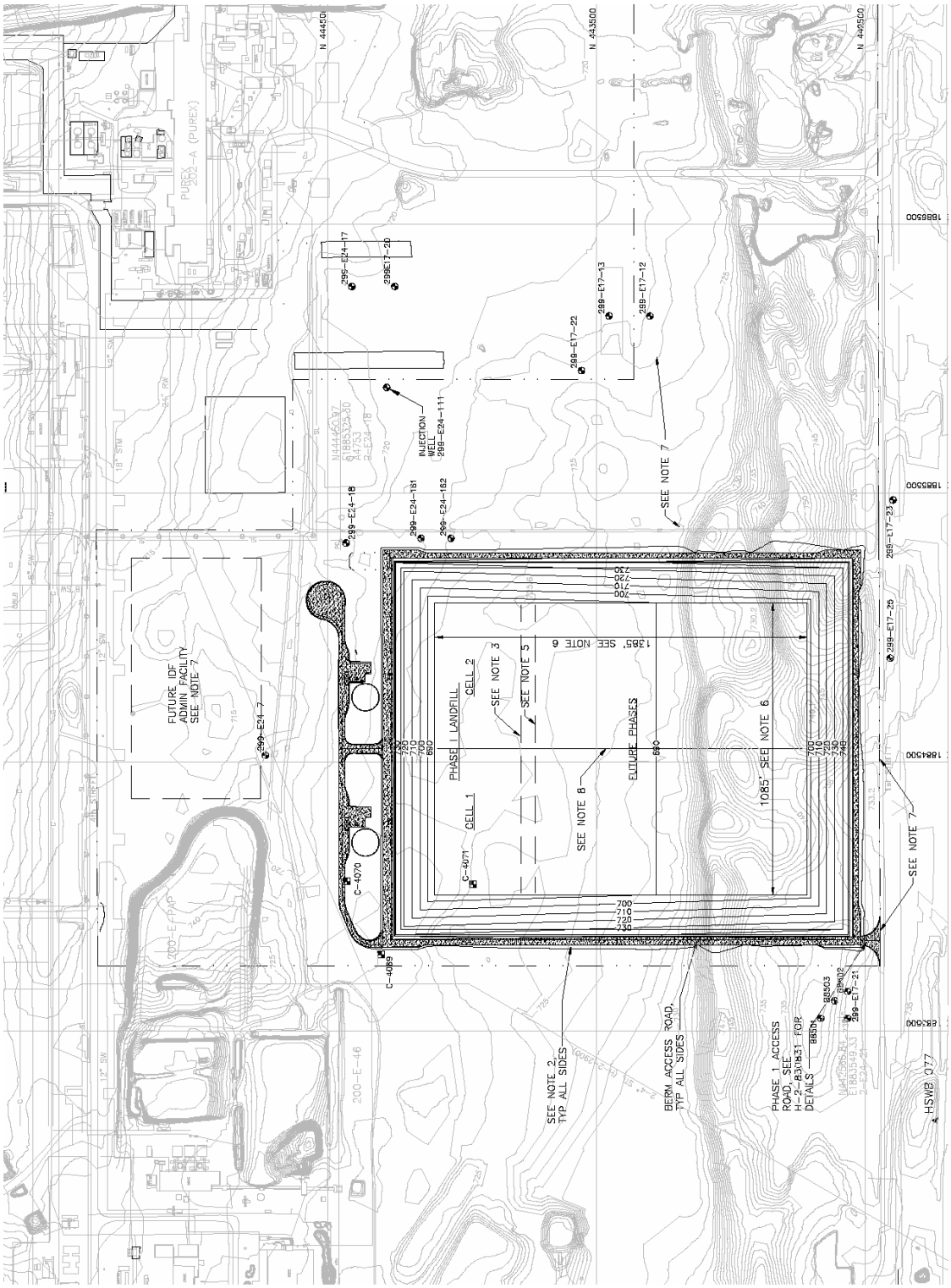

Figure 2.3. Layout of the IDF Facility within the Site

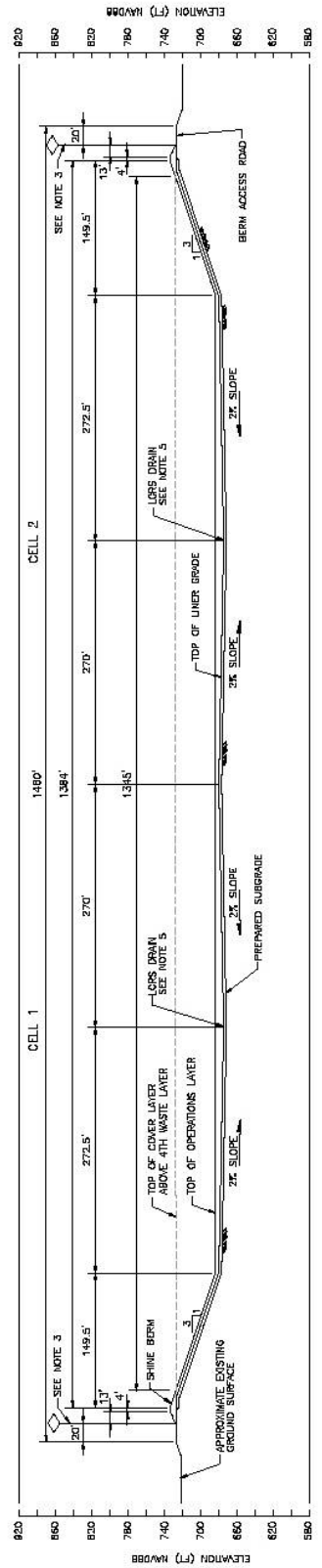

Figure 2.4. East-West Cross-Section through the IDF Trench (from CHG 2003c)

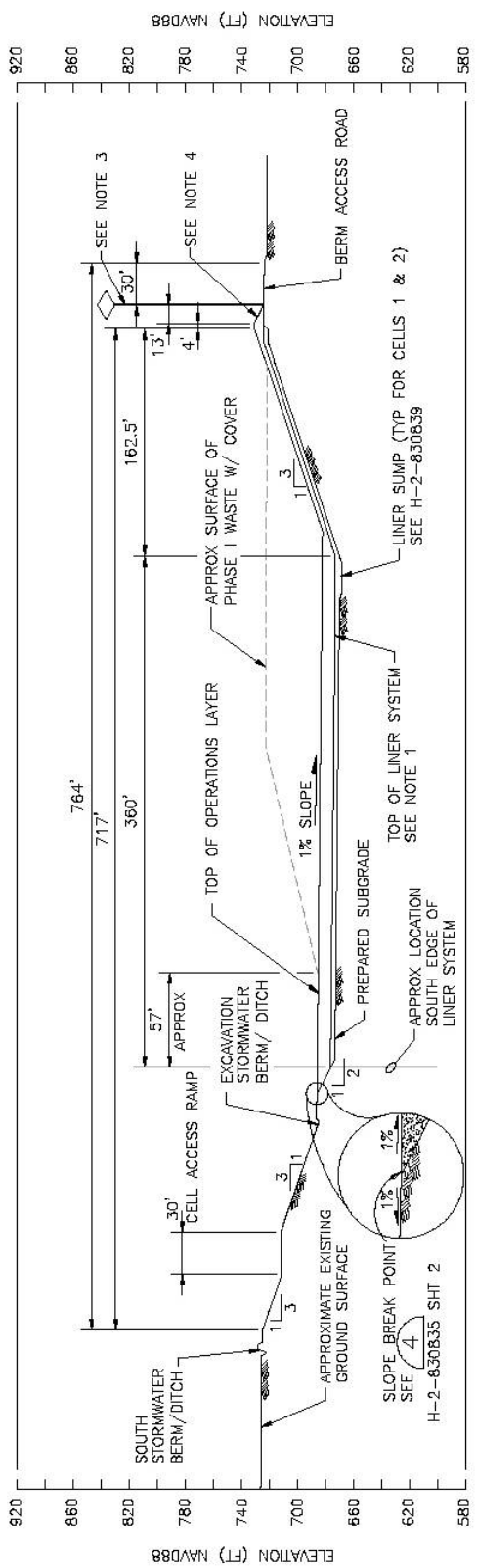

Figure 2.5. North-South Cross-Section through the IDF Trench (from CHG 2003c)

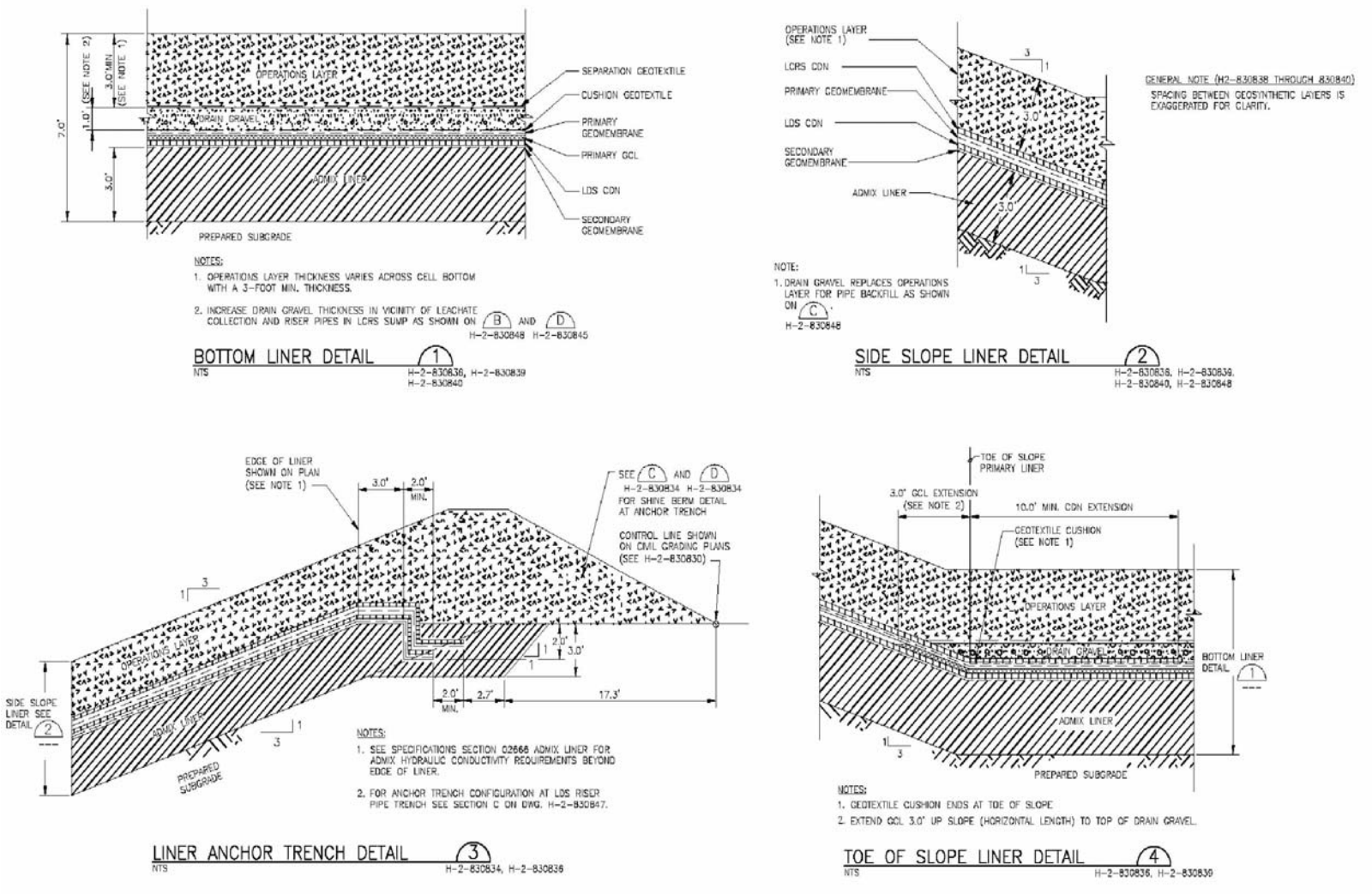

Figure 2.6. Details of IDF Trench Liner (from CHG 2003c)

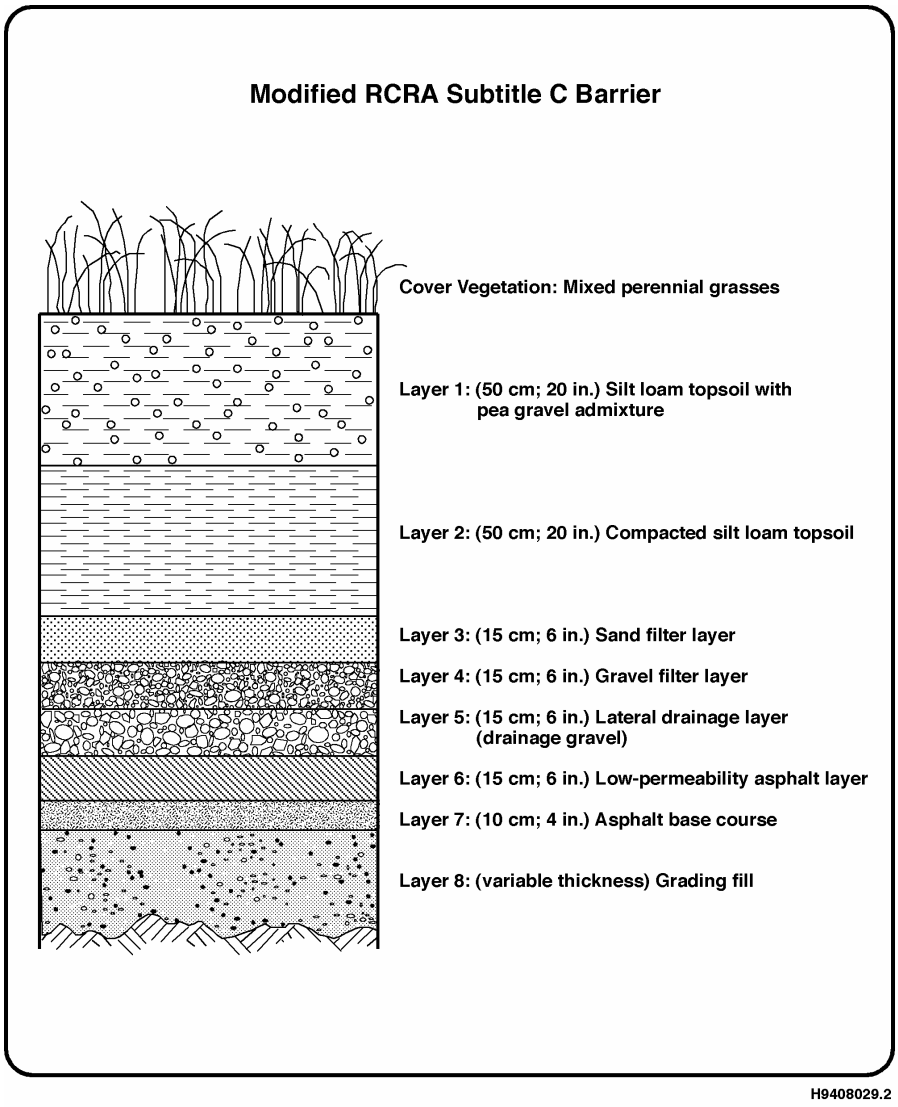

Figure 2.7. Schematic Profile of the Modified RCRA Subtitle C Barrier

The materials currently specified or that may potentially be used in the IDF disposal facility are discussed below.

2.2.1 Surface Cover

A description of each component of the surface cover is given below, taken primarily from DOE (1993a). This section is nearly identical to that presented in Meyer and Serne (1999), but is included here for completeness.

2.2.1.1 Layer 1: Silt Loam Soil with Gravel

This layer consists of 50 cm of sandy silt to silt loam soil (matching the characteristics of such soil from the McGee Ranch area on the Hanford Site) with 15% pea gravel by weight. The design bulk density of this layer is about 1.46 g/cm3. The surface slope is limited to a maximum of 2% (after allowances for settlement and subsidence). The purpose of Layer 1 is to support vegetation and provide maximum storage capacity for precipitation and snowmelt. A large storage capacity in conjunction with evapotranspiration from vegetation will tend to minimize percolation from the cover (recharge). The pea gravel provides resistance to erosion of the silt loam.

2.2.1.2 Layer 2: Compacted Silt Loam Soil

This layer consists of an additional 50 cm of silt loam soil, but without the addition of pea gravel. This layer will be compacted during construction to a design bulk density of about 1.76 g/cm3. The purpose of Layer 2 is to provide water storage capacity for precipitation and snowmelt and support for vegetation. The purpose of the compaction is to reduce the hydraulic conductivity of the layer.

2.2.1.3 Layer 3: Sand Filter

This layer consists of 15 cm of graded sand that is intended to serve, in conjunction with Layer 4, as a filter, preventing the fine particles of Layer 2 from moving into the lateral drainage layer (Layer 6). Particle size requirements for the sand filter were taken from Cedergren (1989) [also cited in Ecology (1987) and EPA (1989)] and are as follows.

Retention Criteria: D_{15} (Filter)/ D_{85} (Filtrate) < 4 to 5

D_{50} (Filter)/ D_{50} (Filtrate) < 25

Permeability Criterion: D_{15} (Filter)/ D_{15} (Filtrate) > 4 to 5

The D values refer to the particle diameters on a particle size distribution curve (e.g., D_{15} is the particle diameter at which 15% of the particles are smaller). The filter material in this case is the sand; the filtrate material is the compacted silt loam. These filtration criteria were developed for applications in earth dams under saturated conditions. They are expected to be conservative for the unsaturated conditions of the ILAW surface cover.

The presence of the relatively coarse textured sand layer immediately beneath the fine textured silt loam will produce a capillary barrier effect at the interface. This effect arises because the unsaturated hydraulic conductivity of the sand will be significantly less than that of the silt loam for a large range of matric potential. Significant flow into the sand layer will not occur until the matric potential at the silt loam-sand interface becomes sufficiently large (close to zero) that water can move into the relatively large pores of the sand (Hillel, 1980). The capillary barrier will, in effect, increase the water storage capacity of the silt loam layers. Its ability to do so will depend on the hydraulic properties of the silt loam and sand materials.

2.2.1.4 Layer 4: Gravel Filter

This layer consists of 15 cm of a graded gravel that functions, with Layer 3, as a filter, preventing the fine particles of Layer 2 from moving into the lateral drainage layer (Layer 6). Particle size requirements for this layer are identical to those of the sand filter (Layer 3), with the exception that the filter material in this case is the gravel and the filtrate material is the sand. No slope is specified for the sand and gravel filter layers. It is assumed that they will be constructed at a 2% slope (as drawn in Figure 2.2) to minimize required thickness of the surface cover.

2.2.1.5 Layer 5: Gravel Lateral Drainage Layer

This layer consists of 15 cm of screened gravel with a required saturated hydraulic conductivity of no less than 1.0 cm/s. This layer will be constructed at a 2% slope. Its purpose is to divert (to the edge of the cover) water that passes through the filter layers and reaches the asphalt layer (Layer 6).

2.2.1.6 Layer 6: Asphaltic Concrete

This layer consists of 15 cm of a durable asphaltic concrete mixture consisting of double-tar asphalt with added sand as binder material, conforming to WSDOT M41-10, Section 9-02.1(4), Grade AR-4000W (WDOT, 1991). The asphaltic concrete will potentially be coated with a spray-applied asphaltic material. This layer will be constructed at a 2% slope. The asphalt layer is intended to function as a low permeability layer and as an inadvertent intruder barrier. As a low permeability layer, analogous to the compacted soil component of a standard RCRA Subtitle C barrier, the asphalt layer should be expected to have a maximum saturated hydraulic conductivity of 10^{-7} cm/s.

2.2.1.7 Layer 7: Asphalt Base Course

This layer serves as a stable base for placement of the asphalt and consists of 10 cm of screened, crushed surfacing material, with 100% passing the 32 mm sieve. The material must conform to WSDOT M 41-10, Section 9-03.9(3) (WDOT, 1991).

2.2.1.8 Layer 8: Grading Fill

This material consists of a well-graded, granular soil mixture, which may include as much as 20% by volume of cobbles measuring no more than 75 mm in the greatest dimension. This material will be used as needed to establish the base for construction of the other cover layers. Backfill material from excavation of the trench may serve as the grading fill.

2.2.1.9 Other Potential Surface Cover Components

A water conditioning layer consisting of quartz sand or crushed glass has been considered as a component of the surface cover. The intent of this layer is to increase the silica content of water that contacts the waste, thus reducing the dissolution of silica in the ILAW glass and decreasing the contaminant flux from the facility. No specifications have been given for this material.

A diversion layer consisting of a sand and gravel capillary barrier may potentially be used in the final design of the facility cover. The diversion layer would be used as an alternative to, or in addition to, the asphalt low permeability layer and would consist of a well-graded sand overlying a well-graded gravel. The diversion layer would likely be constructed at a 2% slope, corresponding to the other surface cover components. Specifications for the diversion layer component have not been given.

2.2.2 Trench Liner

Liner details are shown in Figure 2.6. Complete specifications for the liner components are given in CHG (2003c). A summary of the liner components and specifications is given here.

2.2.2.1 Liner Subgrade

The liner will be placed on a prepared subgrade consisting of native soils compacted to 95 percent relative compaction.

2.2.2.2 Admix Liner

The admix liner is intended to provide a low permeability barrier against the infiltration of liquids or contaminants. The admix liner consists of a moisture-conditioned admixture of natural base soil obtained from the IDF site and bentonite, compacted to achieve a hydraulic conductivity of no more than 10^{-7} cm/s. The base soil will be less than 1 percent by weight rocks greater than 2.54 cm diameter and will be at least 20 percent by weight finer than 0.075 mm (No. 200 U.S. Sieve). The admixture will consist of 12 percent by dry weight commercially-prepared bentonite. Minimum required thickness of the admix liner is three feet.

2.2.2.3 Geomembrane Liners

The primary and secondary geomembranes are 60 mil textured High Density Polyethylene (HDPE). Specific requirements for physical, mechanical, and seam properties are given in CHG (2003c).

2.2.2.4 Geosynthetic Clay Liner

The bottom liner includes a geosynthetic clay liner (GCL) between the HDPE geomembranes. The low permeability component of the GCL is bentonite; the permeability to water of the GCL is required to be no greater than $5x10^{-9}$ cm/s.

2.2.2.5 Other Geosynthetic Materials

Various other geosynthetic materials are specified as components of the liner. These include geotextiles for the purpose of separating soil layers (such as the operations layer and the drain gravel layer) and for the purpose of cushioning the geomembrane liner (from the drain gravel layer). A geosynthetic composite drainage network (CDN) is specified above one or both of the geomembrane liners to facilitate drainage to the sumps. The geotextiles should have a minimum impact on the movement of water. The required transmissivity of the CDN is $5x10^{-4}$ m^2/s.

2.2.2.6 Drain Gravel

A one-foot-thick layer of subrounded to rounded gravel is specified for the bottom liner of the trench above the primary geomembrane liner. This layer is intended to provide drainage to the sumps. The drain gravel must have a hydraulic conductivity greater than 0.1 cm/s.

2.2.3 Operations Layer

The waste packages will be placed on an operations layer consisting of excavation spoils and borrow materials with a maximum particle size of two inches and no more than 25 percent by weight finer than 0.075 mm diameter.

2.2.4 Waste Package Materials

These materials include the waste forms themselves as well as the materials of the waste packages and the filler material used to fill the void space within the waste packages. As stated above, the IDF is designed to accept several categories of waste. The characteristics of the disposed WTP melter packages are currently unspecified. In the IDF risk assessment (Mann et al. 2003a) it was assumed that the melters contained some volume of waste glass and that the melters were grouted into steel overpacks 4.38 x 5.29 x 5.29 m (for high level waste melters) or 4.86 x 6.79 x 9.28 m (for low activity waste melters). The space between waste containers will be filled with a porous backfill material such as sand obtained from the trench excavation.

2.2.4.1 ILAW Glass and Container

The current design calls for the molten ILAW glass to be poured into steel cylindrical containers (1.22-m diameter by 2.29-m tall), with 85 percent of the container volume filled by the ILAW waste glass. The void space within ILAW containers is expected to be filled with an inert material, such as sand from a local source. Significant fracturing of the glass is anticipated, particularly where the glass forms an edge. In previous PA simulations, fracturing has been assumed to increase the surface area of the glass by about ten times. The steel container is expected to corrode and have little impact on waste form release or flow and transport (Mann et al. 2001).

2.2.4.2 LLW/MLLW and Container

It is anticipated that the MLLW/LLW will be packaged in containers composed of steel, wood, or concrete (Wood et al. 1996). For such packages disposed in the Hanford Solid Waste Burial Grounds, void fractions are required to be no greater than 10 percent, although there are no requirements addressing compressibility (Puigh 2004). According to Mann et al. (2003a), there are no performance requirements for the waste form or the waste package for most LLW. For MLLW, waste package and waste form performance is generally provided by concrete containers or by grouting the waste. In past PAs (Wood 1995,1996), relatively simple, conservative models of waste form release have been used. These simple models do not require the unsaturated hydraulic properties of the LLW/MLLW waste forms.

2.2.4.3 WTP Melters and Overpack

The waste package designs for the WTP melters have not been specified. Puigh (2004) describes the current assumptions regarding the content and dimensions of these waste packages. The overpacks are assumed to consist of carbon steel boxes with the steel eight inches thick for the high-level waste (HLW) melters and one inch thick for the LLW melters. Overall dimensions of the waste packages, including overpacks are assumed to be 5.29 m square by 4.38 m in height for the HLW melters and 6.79 by 9.38 by 4.86 m high for the LLW melters. It is assumed that the melter will contain a residual glass waste with a maximum glass volume of 5.75 m^3 for the HLW melters and 14.52 m^3 for the LLW melters (density of the cold glass is assumed to be 2.6 g/cm^3. It is also assumed that the melters will be grouted into their overpacks.

2.2.4.4 Supplemental ILAW Waste Forms

Alternative technologies, supplemental to the baseline vitrification process, are being considered for producing ILAW. A preliminary risk assessment for the disposal of supplemental ILAW waste forms at the IDF was recently completed (Mann et al. 2003b). This risk assessment considered three supplemental technologies: bulk vitrification, cast stone, and steam reformer. For the IDF PA, it is assumed that all WTP supplemental technology waste is processed by bulk vitrification (Puigh 2004), a process that involves mixing LAW, soil, and glass-forming chemicals and melting them in a large container (which becomes the waste package) by electrical resistance heating. The bulk vitrification waste package design has not been specified. It is assumed for the IDF PA that the waste will be contained within a steel box with dimensions of 7.5 by 2.4 by 2.8 m in height. The steel container was assumed to be lined with an insulating layer of quartz sand in the risk assessment (Mann et al. 2003b). Current tests of the bulk vitrification process use a series of refractory materials to line the container: insulating foam board, sand, and a cast (brick-like) material that is placed adjacent to the LAW/soil/glass-forming chemicals mixture[1]. For the IDF PA, it is anticipated that the resulting glass material will be assumed to have uniform physical properties (without the froth layer discussed in Mann et al. 2003b). Any void space in the waste package after the bulk vitrification product has cooled is assumed to be filled with sand soil obtained from a local source.

2.2.5 Backfill

Backfill within the trench will consist of excavation spoils and borrow materials. CHG (2003c) specifies such backfill (referred to as Earthfill) to have a maximum particle size of four inches. For the fill

[1] P. Sederberg, AMEC Earth & Environmental, Inc., Richland Washington, May 2004, personal communication.

around and between waste packages, the maximum particle size may be less to limit the potential formation of void spaces. As a result of the excavation, re-emplacement, and compaction, the backfill hydraulic properties are expected to differ from the properties of the naturally occurring sediments. The backfill is likely to be more homogeneous and isotropic.

3.0 Required Properties and Parameters of Near-Field Materials

This section provides a brief description of the basic properties and parameters required to model unsaturated flow and nonreactive contaminant transport in the near-field environment of the IDF disposal facility. Additional parameters required to model reactive transport are discussed in Krupka et al. (2004) and Pierce et al. (2004). This section is largely taken from Meyer and Serne (1999) with some modifications to update references and add relevant material.

3.1 Particle Size Distribution

The particle size distribution (PSD) is typically presented as the cumulative fraction by weight of particles whose mean diameter is less than a specific value. This physical property is useful for classifying soils (e.g., sand, silt loam), but is not typically used directly in modeling. Those particles greater than 2 mm in diameter are often removed from the sample before measuring the particle size distribution using standard methods (ASTM D422-63; Gee and Or 2002). For ILAW PA purposes, however, the fraction greater than 2 mm should be included in the particle size distribution or recorded as a gravel percentage.

In the absence of a direct measurement of water retention (see Section 3.5), the particle size distribution can be used to estimate water retention by assuming the particle size distribution reflects the pore size distribution (Arya and Paris 1981; Arya et al. 1999a). Particle size distribution has also been related to the unsaturated hydraulic conductivity function (Arya et al 1999b).

3.2 Particle Density

Particle density (ρ_p) is the mass of solids in a sample divided by the volume of the solids. It is typically used to calculate porosity. The sample fraction with a nominal diameter less than 2 mm may be used in the measurement of particle density. Flint and Flint (2002a) discuss methods to estimate particle density.

3.3 Bulk Density

The dry bulk density (ρ_b) is the mass of solids in a sample divided by the total (bulk) volume of the sample. The total volume includes the volume occupied by the solids, water (or other liquid), and air. Due to the potential for compaction during sampling, bulk density measured in the laboratory may vary from that measured in situ. Bulk density is often used to calculate porosity and retardation coefficients. Some techniques for estimating water retention and hydraulic conductivity may also use the bulk density. Grossman and Reinsch (2002) discuss methods to estimate bulk density.

3.4 Porosity

Porosity (ϕ) is the volume of voids in a sample (the air- and liquid-filled volume) divided by the total volume of the sample. It is typically calculated using measured values of particle and dry bulk densities.

$$\phi = 1 - \rho_b/\rho_p \quad (3\text{-}1)$$

The porosity can also be measured directly (Flint and Flint 2002b). For some materials a fraction of the void space is disconnected and cannot take part in flow. For these materials, a distinction may be made between the total porosity and the effective porosity (also refered to as the connected or apparent porosity). The effective porosity is always less than or equal to the total porosity.

3.5 Water Retention

Water retention [$\theta = f(\psi)$]in a porous medium refers to the relationship between water content and matric potential. Volumetric water content (θ) is the volume of water in a sample divided by the total volume of the sample. The matric potential (ψ) represents the capillary and adsorptive forces that attract and bind water to the soil matrix. (Matric potential is also referred to as soil water pressure or negative soil water tension.) A variety of methods are available to obtain water retention data (Dane and Topp 2002). In some cases, laboratory measurements of water retention have been conducted on samples for which the gravel fraction (particle diameter > 2 mm) has been removed. The water contents obtained on such samples should be corrected for the gravel content (Bouwer and Rice 1983) before estimating the parameters of a water retention model.

Water retention is typically represented in simulation codes using one of a number of water retention models that have been presented in the literature. In this report, the model proposed by van Genuchten (1980) is used:

$$S_e(\psi) = [1 + (\alpha\psi)^n]^{-m} \quad (3\text{-}2)$$

where

ψ = matric potential

S_e = effective saturation = $\frac{\theta - \theta_r}{\theta_s - \theta_r}$, $0 \le S_e \le 1$

α = curve fitting parameter related to air entry pressure

n, m = curve fitting parameters related to pore size distribution; the relationship, m=1-1/n, is often assumed

θ_r = residual (or irreducible) water content

θ_s = saturated water content.

The saturated water content is often assumed to be equal to porosity. It has been observed in laboratory and field measurements, however, that soils often cannot be saturated to the full porosity. This effect is more pronounced in the field, presumably because of the greater variation in soil structure and the inability to carefully control wetting. For this reason, θ_s is sometimes a fitted parameter, in which case

it represents a field-saturated water content. Klute (1986) states that field-saturated water content is typically 80 to 90% of the porosity.

The residual water content is interpreted here as an empirical parameter and thus is generally a fitted parameter. This interpretation is a subject of debate (Nimmo 1991; Luckner et al. 1991). At very low matric potentials (large negative values), the van Genuchten model may provide a poor representation of water retention. Alternative models have been proposed that improve the fit at low water contents (Rossi and Nimmo 1994; Fayer and Simmons 1995). Because water contents in the ILAW disposal facilities and the surrounding soils are expected to be low, accurate representation by the water retention model may be important. This is especially true if diffusion dominates the transport of contaminants and a water-content-dependent diffusion coefficient is used.

The remainder of the parameters in the van Genuchten water retention model are fitting parameters, estimated using measured or inferred water retention data.

There are many water retention models that could be used. Although the parameters in the van Genuchten model are related to the parameters used in other models (e.g., Lenhard et al. 1989), the transformation from one to the other is not always straightforward. Caution should be exercised in using the results presented in this report with water retention models other than the van Genuchten model.

Water retention in soils and sediment exhibits hysteresis: the observed water content at a given matric potential depends on whether the soil is being wetted or is drying. Models have been developed for describing this hysteresis (e.g., Parker and Lenhard 1987; Lenhard and Parker 1987), but the data on which the parameters of hysteresis can be estimated are often not available. Hysteresis is likely to be most important near the ground surface where water content changes with time will be the largest. In the deeper materials (below the cover), water content changes will be less significant and hysteresis effects are not anticipated to be significant.

3.6 Saturated Hydraulic Conductivity

Darcy's Law is used in models of subsurface flow to relate water flux to the potential gradient. Under saturated conditions, the proportionality constant in this relationship is the saturated hydraulic conductivity (K_s). Measurements can be made using a variety of methods (Dane and Topp 2002). Saturated hydraulic conductivity may exhibit anisotropy: a value that depends on the direction in which it is measured. Data on anisotropy are typically not available. Hydraulic conductivity anisotropy is not anticipated to be significant in any single near-field material. At a scale that encompasses multiple near-field materials that have contrasting properties, anisotropy should be considered.

Saturated hydraulic conductivity measurements are often made on small-scale laboratory samples. Because of the variability in natural materials, these small-scale measurements should not be interpreted as field-measured hydraulic conductivity values, which are typically larger. Values used in numerical models should represent the scale of the numerical grid size. The appropriate scaling methods for deriving model values of saturated hydraulic conductivity from laboratory measurements is currently a matter of scientific debate. Because the near-field materials will be relatively homogeneous, the scaling issue is anticipated to be less important than for the naturally occurring sediments.

3.7 Unsaturated Hydraulic Conductivity

Under unsaturated conditions, the water flux occurring through a porous material in response to a specified potential gradient is strongly dependent on the water content of the material. The unsaturated hydraulic conductivity [$K = f(\theta, \psi)$] describes this dependence. Direct measurement of the unsaturated hydraulic conductivity as a function of water content is possible using a variety of methods (Dane and Topp 2002). The expense of acquiring such data, however, means that it is often not available. More typically, the unsaturated hydraulic conductivity relationship is estimated using water retention and saturated hydraulic conductivity measurements and adopting a particular model (e.g., Mualem 1976). Hopmans et al. (2002) discusses indirect estimation of unsaturated hydraulic conductivity using inverse methods; these methods also requires adopting a specific model.

The unsaturated hydraulic conductivity model used in this report is the model derived by van Genuchten (1980) using the relationship of Mualem (1976). This model can be written either in terms of the water content or the matric potential.

$$K(S_e) = K_s \sqrt{S_e}\,[1-(1-S_e^{1/m})^m]^2 \tag{3-3}$$

$$K(\psi) = K_s \frac{\{1-(\alpha\psi)^{n-1}[1+(\alpha\psi)^n]^{-m}\}^2}{[1+(\alpha\psi)^n]^{Lm}} \tag{3-4}$$

Parameters in these equations are as defined for the water retention model and can be estimated using both water retention and unsaturated hydraulic conductivity data when available. The parameter L in the exponent of the denominator of Equation 3-4 accounts for pore connectivity and tortuosity effects. A value of $L = 0.5$ is typically assumed although fitted data often yield values significantly different (e.g., Schaap and Leij 2000).

Anisotropy in the unsaturated hydraulic conductivity is known to be dependent on saturation (Zaslavsky and Sinai 1981) with the anisotropy factor increasing as saturation is reduced (Stephens and Heerman 1988). Zhang et al. (2003) provide a model for representing the saturation-dependent anisotropy by assigning a directional dependence to L.

Khaleel et al. (1995) found that the van Genuchten-Mualem model did not provide accurate estimates of unsaturated hydraulic conductivity for Hanford sediments at low water contents when these estimates were based solely on water retention data and a saturated hydraulic conductivity measurement. This condition may be explained by observing that the saturated hydraulic conductivity for these relatively coarse materials is dominated by large pores, whereas the unsaturated hydraulic conductivity appears to be dominated by small pores. Khaleel et al. (1995) recommended the use of at least one direct measurement of hydraulic conductivity at a low water content as a match point.

3.8 Dispersivity

Dispersivity (λ), when multiplied by the pore water velocity, yields the mechanical dispersion coefficient, which relates the dispersive solute flux to the solute concentration gradient. Dispersivity is

generally larger in the direction of flow than in transverse directions and it is also scale dependent. Khaleel et al. (2002) provides a discussion of the issues related to scale-dependent dispersion with particular application to modeling flow and transport in the far-field IDF environment. Because of the smaller scale and the relative homogeneity within a given material, this issue is likely to be less important for the near-field materials.

Field measurements of dispersivity are rare and small-scale laboratory measurements have only marginal utility in estimating field values. In the absence of data, dispersivity values are often based on simple guidelines related to the size of the computational elements in numerical simulation codes.

3.9 Diffusion Coefficient

The diffusion coefficient is the proportionality factor in Fick's law that relates the diffusive transport flux to the gradient in solute concentration. Diffusion results in mass transport from regions of high solute concentration to regions of lower concentration and occurs as a result of the random thermal motion (Brownian motion) of molecules and atoms. Diffusive transport in a dilute water solution is quantified by the free-water diffusion coefficient, D_f. For most simple aqueous species D_f is about 10^{-5} cm^2/s (10^{-9} m^2/s). Kemper (1986) provides a table of diffusion coefficients of common ions in water; values range from approximately 4.8 x 10^{-6} to 1.6 x 10^{-5} cm^2/s at 15 ºC (see also Flury and Gimmi 2002).

In the constrained geometry of a porous medium, the diffusion coefficient is reduced compared to the diffusion coefficient in free aqueous solution. The intrinsic diffusion coefficient for a species within a saturated porous medium, D_i, can be expressed as

$$D_i = D_f \phi \delta / \tau \tag{3-5}$$

where δ = a constrictivity factor

$1/\tau$ = a tortuosity factor.

The intrinsic diffusion coefficient has also been referred to as the effective diffusion coefficient.

The constrictivity factor in Equation 3-5 represents a reduction in diffusion due to the constricted flow path caused by small pores and pore throats in the porous medium. The tortuosity factor represents a reduction in diffusion due to the increased path length taken by solute molecules in traveling through the porous medium. The tortuosity factor is given by $1/\tau = (L_s/L_e)^2$, where L_e is the length of the tortuous path and L_s is the straight-line path length (Porter et al. 1960).

In a saturated porous medium, the cross-sectional area available for diffusion in the aqueous phase is reduced by the volume fraction of the void space. This fraction will be the total porosity, ϕ, if all porosity in the porous medium is interconnected and can thus contribute to contaminant diffusion. If there are pores that do not contribute to diffusion (such as dead end pores), the porosity appearing in Equation 3-5 will be less than the total porosity. In unsaturated porous media, Equation 3-5 must be modified to account for the additional reduction in cross-sectional area available for diffusion as a result of the reduced volumetric water content.

In practice, it is difficult to directly measure or reliably estimate the constrictivity and tortuosity factors. As a result, the intrinsic diffusion coefficient is frequently modeled empirically as a function of the porosity and/or water content (e.g., Millington 1959, Papendick and Campbell 1980, Kemper and Van Schaik 1966). The value of the diffusion coefficient can vary significantly depending on which of the empirical relationships is used, particularly at low water contents. Under the appropriate conditions, these differences may have a significant impact on predicted contaminant concentrations. Differences are potentially greatest for diffusion-dominated transport, such as occurs within the IDF near-field environment. A generalization of the power function model proposed by Campbell (1985) is recommended for use in the IDF PA. This model has the form

$$D_i(\theta) = \mathrm{a}\, D_f\, \theta^{\mathrm{b}} \tag{3-6}$$

where a and b are empirical coefficients. Appropriate values of these coefficients for use in the IDF PA are discussed in Chapter 5.

The chemical contributions to diffusion can potentially be quite varied and significant. If we assume a very simple chemical process, i.e., reversible surface adsorption having fast kinetics and a linear isotherm (adsorption proportional to the concentration in solution via a fixed constant, K_d), then diffusion of a reactive contaminant can be characterized by an apparent diffusion coefficient, D_a,

$$D_a = D_i / (\theta + \rho_b K_d) \tag{3-7}$$

Estimated values of K_d for a given constituent and sediment can be obtained from the geochemistry data package (Krupka et al. 2004).

4.0 Best-Estimate Values for Hydraulic Parameters of IDF Near-Field Materials

This section contains best-estimate values for the hydraulic parameters of the near-field materials to be used in performance assessment analyses of the IDF disposal facility. The best-estimate values are updates of the values previously presented in Meyer and Serne (1999). A description of the source of these values is included for those parameters that have been updated and for any new materials. Parameter values given in Meyer and Serne (1999) were judged to be adequate for a number of the materials and these parameters are not discussed here. Please refer to the Meyer and Serne (1999) for the technical basis of these parameter values. For the sake of completeness, however, all parameter values are included in the summary table.

In determining the best-estimate parameter values it has been assumed in most cases that the saturated volumetric water content is equal to the porosity. This assumption was made to avoid the application of an arbitrary factor to account for field saturation in such disparate materials as gravel, fractured glass, and concrete. In those cases where a model was fit to water retention data, the saturated water content was a fitted parameter and may be less than the porosity. Best-estimate values for transport parameters are discussed in Chapter 5. Information on parameter uncertainty and changes in parameter values over time is discussed in Chapter 6.

4.1 Surface Cover Materials

In the most recent PA analysis conducted for the disposal of ILAW (Mann et al. 2001), the surface cover was not explicitly simulated. (This was also the case for previous versions of the ILAW PA.) Instead, a piece-wise steady-state water flux through the surface cover was assigned based on data and analyses described in Fayer et al. (1999). Meyer and Serne (1999) nonetheless presented best-estimate parameter values for the components of the surface cover. The only component of the surface cover for which the best-estimate parameters are updated here is the compacted silt loam.

4.1.1 Compacted Silt Loam

The water retention parameter values for this material were previously estimated using water retention data measured on silt loam samples compacted to a bulk density of 1.37 g/cm^3. These water retention data were adjusted for the effect of increasing the bulk density to 1.76 g/cm^3 (the value for this material specified in DOE [1993a]) using the particle size – water retention relationship given in Arya and Paris (1981).

Estimates of the water retention parameters for the compacted silt loam component of the surface cover were improved by making laboratory measurements on compacted samples of silt loam soil obtained on the Hanford Site. The surface cover design calls for the 0.5-m layer of silt loam to be compacted to 90% of optimum dry density with the estimated in-place bulk density given as 1.76 g cm^{-3}. Fayer et al. (1999) reported that a Warden silt loam soil could not be compacted to an in place bulk density greater than 1.6 g/cm^3 in a lysimeter study. In addition, DOE (1993b) reported a maximum dry

density of 1.75 g/cm^3 for the McGee Ranch silt loam soil. A bulk density of 1.58 g/cm^3 is 90% of this maximum for the McGee Ranch silt loam. Water retention measurements were made on three samples of silt loam soil packed to a bulk density of 1.58 g/cm^3 using the method of Lenhard and Parker (1988) for capillary pressures between 0 and 200 cm and using a pressure chamber apparatus for pressures of 1000 and 3000 cm. Both nonhysteretic and hysteretic water retention measurements were conducted. Hysteresis was significant and should be considered when modeling the compacted silt loam (and silt loam – gravel admix) component of the surface cover. Unsaturated hydraulic conductivity was also measured on two samples packed to a bulk density of 1.63 g/cm^3 using a steady-state centrifugation method (ASTM D6527-00).

Parameters of the van Genuchten model (Equations 3-2 and 3-3/3-4) were fit to the compacted silt loam data using nonlinear least squares regression. The hysteretic data was fit to the model of Parker and Lenhard (1987) and Lenhard and Parker (1987). This model uses similar expressions to Equation 3-2, except for two differences. The model accounts for entrapped air using a parameter, θ_{at}, which is the maximum amount of air entrapment when the initial condition is air-dry. In addition, instead of a single α parameter, two α's are used: one for describing the water drainage relation ($^d\alpha$) and one for describing water imbibition ($^i\alpha$). Based on the analysis of the experimental data[2], the following best-estimate parameter values (for the hysteretic model) are proposed for the compacted silt loam. The best-estimate value for the air entrapment parameter is $\theta_{at} = 0.03$.

Table 4.1. Best-Estimate Parameter Values for Compacted Silt Loam

ρ_p (g/cm^3)	ρ_b (g/cm^3)	θ_s	θ_r	$^d\alpha$ (cm^{-1})	$^i\alpha$ (cm^{-1})	n	K_s (cm/s)
2.72	1.58	0.39	0.09	0.006	0.014	1.92	5.2×10^{-5}

4.2 Trench Liner Materials

The proposed design of the ILAW disposal facility at the time Meyer and Serne (1999) was written involved the placement of the ILAW waste packages within a concrete vault constructed within a trench. Meyer and Serne (1999) did not include any liner components in their analysis. In the 2001 ILAW PA (Mann et al. 2001) the concrete vault was not considered in the PA simulations. That is, the performance of the facility was evaluated assuming that the disposal facility consisted solely of the ILAW waste form surrounded by backfill. The contaminated water at the lower extent of the backfill traveled directly into the upper vadose zone. If the simulations for the 2005 IDF PA are conducted in a similar way, the analysis will be assuming that the life of the trench liner will be insignificant with respect to the time-frame for corrosion of the waste form and that a degraded liner will not impact flow and transport.

[2] Lenhard, R.J. and P.D. Meyer. 2000. "Hydraulic and Diffusion Property Measurements of ILAW Near-Field Materials: FY00 Status Report," Letter Report to CH2MHill Hanford Group, Inc., November 3, 2000, Pacific Northwest National Laboratory, Richland Washington.

The current design of the trench liner includes a number of low permeability components: the admix liner, two geomembrane liners, and a geosynthetic clay liner. Assuming that these components do not impact the long-term performance of the IDF facility is a conservative assumption, as long as the so-called bathtub effect does not occur. This effect would occur if water infiltrates into the facility faster than it is transmitted through the liner (or removed from the liner via the sumps). The upper bound recharge rate through the Modified RCRA C cover is estimated to be 1.3×10^{-9} cm/s (Fayer and Szecsody 2004). This is less than the design hydraulic conductivity of the admix liner and is comparable to the geosynthetic clay liner permeability. The design permeability of the geomembranes is lower and thus the potential for the accumulation of water above the liner depends on the quality and longevity of the geomembrane liners.

Best-estimate unsaturated hydraulic parameters are not provided for the trench liner components since the assumption that the liner has no impact on flow and transport is likely to be conservative. A sensitivity case can be run to determine the potential impact of the bathtub effect on waste form release and facility performance.

4.3 Operations Layer

It is recommended that this material be assumed to have the same hydraulic properties as the high-density backfill (see Section 4.52.2.5).

4.4 Waste Package Materials

4.4.1 ILAW Glass

It is anticipated that the glass waste will be poured into steel packages and allowed to cool whereupon significant fracturing is anticipated, particularly on the exterior of the glass and along edges. It was assumed in the 2001 ILAW PA (Mann et al. 2001) that the fracturing will be sufficient to allow the glass waste to be treated as an effective porous medium, instead of a fractured medium, and thus the parameters are the same as for the other materials. All porosity in the glass will reside in the fractures (i.e., the glass matrix has no porosity). Total porosity is anticipated to be small – on the order of a few percent.

Meyer and Serne (1999) based the ILAW glass hydraulic properties on expected physical features of the glass. In order to improve on these estimates, samples of simulated ILAW glass (the glass known as HAN-28) were produced and fractured by rapid cooling. A photograph of the top of one of these samples is shown in Figure 4.1. Indirect methods must be used to characterize small-sized fractures in materials. A common approach is to use mercury porosimetry, which involves injecting mercury into a porous medium under controlled pressures. Based on the volume of mercury injected over a change in pressure, the volume of fractures with known effective radii can be determined. In the petroleum industry, the pore-size distribution of consolidated rock cores is typically determined by mercury porosimetry. The diameter of the rock cores used in mercury porosimetry is generally less than one inch (i.e., 2.54 cm). Because of the one-inch size limitation associated with commercially available mercury porosimetry, another measurement procedure needed to be developed that was suitable for larger-sized glass cylinders such as the glass samples used here.

The approach adapted relies on methods used in soil science to characterize the relations between fluid pressures and saturations. Theoretically, wetting fluid will remain in pores/fractures until the difference between the nonwetting and wetting fluid pressures (i.e., the capillary pressure) exceeds a critical value. The relationship between capillary pressure and size of pores/fractures is based on Laplace's equation of capillarity

$$P_c = \sigma\left(\frac{1}{R_1} + \frac{1}{R_2}\right) \tag{4-1}$$

where P_c is the capillary pressure, σ is the interfacial tension between the nonwetting and wetting fluids, and R_1 and R_2 are radii of curvature of the fluid interfaces in orthogonal directions. The radii of pores or fractures can be determined from the radii of curvature of the fluid interfaces in the pores/fractures and knowledge of the angle that the wetting fluid makes with the solid surfaces (i.e., contact angle). For simplicity, it is common to assume that the contact angle the wetting fluid makes with the pore/fracture walls is zero, which makes the radii of curvature of the fluid interface equal to the pore/fracture radii. This assumption is common because it is difficult to characterize contact angles in the complex pore/fracture geometry that occurs in porous media.

Assuming that the contact angle is zero and the length of the fracture (R_1) is much larger than the diameter (i.e., opening) of the fracture ($2R_2$), then Equation 4-1 reduces to

$$P_c = \frac{2\sigma}{D_f} \tag{4-2}$$

where D_f is the diameter of the fracture. Using this theory, measurements of air-water saturation-pressure relations can be used to characterize the effective size distribution of fractures in the glass cylinders.

Two different apparatuses were used to measure saturation-pressure relations on three glass cylinders.[3] For capillary pressures greater than 100 cm of water height, a pressure chamber was used (Dane and Hopmans 2002). Measurements were conducted at capillary pressures of 200, 400, 600, 800, and 1,000 cm of water height. For capillary pressures less than 100 cm of water height, a tension table was used (Romano et al. 2002). Water saturations were measured at capillary pressures of 2, 10, 20, 30, 40, 50, and 60 cm of water height. A tension table allows for greater sensitivity in conducting measurements, but can only be employed for lower capillary pressures.

From Equation 4-2, it can be seen that a unique effective fracture diameter corresponds to a capillary pressure, provided hysteresis is neglected. The difference in water mass between two saturation-pressure

[3] Lenhard, R.J. and P.D. Meyer. 2000. "Hydraulic and Diffusion Property Measurements of ILAW Near-Field Materials: FY00 Status Report," Letter Report to CH2MHill Hanford Group, Inc., November 3, 2000, Pacific Northwest National Laboratory, Richland Washington.

measurements is therefore related to the volume of fractures with sizes corresponding to the capillary pressures. In differential form, the effective fracture diameter distribution can be determined from

$$\frac{dS_e}{dD_f} = \frac{dS_e}{d\left(1/P_c\right)} \tag{4-3}$$

To solve Equation 4-3, one needs to express S_e in terms of P_c, which was accomplished here using the van Genuchten water retention function. The effective fracture diameter distribution for the three glass samples was estimated.

Because of potential errors associated with boundary effects (between the glass and the steel cylinder), the difference between the water mass at a capillary pressure of 2 cm of water height and dry conditions was used to represent the total fracture volume in the glass. A water mass density of 0.998 g/cm^3 was used to convert the water mass measurements into volumes. Using the 2-cm capillary pressure measurements to calculate the total volume of fractures and using the average total volume of the glass cores (core diameter approx. 5 cm; core height approx. 6 cm), the total porosity of the glass fractures was estimated to be 2 or 3% of the total glass volume for each of the samples. This porosity is consistent with the expected porosity of the ILAW glass.

By calculating the difference in water mass between the capillary pressure measurements and employing Equation 4-2 to relate capillary pressure to a fracture diameter, the volume of fractures between fracture sizes was determined. An air-water interfacial tension of 0.07 N m^{-1} was used in these calculations. The fracture volumes for the three samples are given below. This information may be useful in the event that the actual fracture characteristics of the ILAW glass are measured. A model could then be used to estimate bulk effective hydraulic properties from knowledge of the fracture characteristics. Such a model has been developed for potential use in the IDF PA[4].

The van Genuchten model was fit to the pressure-saturation data for the fractured glass samples. Geometric mean values are given below as the best-estimate parameter values. The saturated hydraulic conductivity of these samples was not measured because of the void space between the boundary of the glass and the steel cylinder.

[4] Freedman, V.L. E.J. Freeman, and P.D. Meyer. 2002. Status Report for ILAW Near-Field Hydrology Efforts Performed in FY02, Modeling Methodology for Determining the Unsaturated Hydraulic Properties of ILAW Glass, Letter Report to CH2MHill Hanford Group, Inc., September 30, 2002, Pacific Northwest National Laboratory, Richland Washington.

Table 4.2. Volume of Fractures as a Function of Fracture Diameter

Fracture Diameters	Glass Samples		
	1	2	3
7.16×10^{-4} to 1.43×10^{-4} m	0.07 cm^3	0.06 cm^3	0.17 cm^3
1.43×10^{-4} to 7.16×10^{-5} m	0.68 cm^3	0.50 cm^3	1.36 cm^3
7.16×10^{-5} to 4.77×10^{-5} m	0.21 cm^3	0.24 cm^3	0.37 cm^3
4.77×10^{-5} to 3.58×10^{-5} m	0.12 cm^3	0.10 cm^3	0.08 cm^3
3.58×10^{-5} to 2.86×10^{-5} m	0.22 cm^3	0.19 cm^3	0.20 cm^3
2.86×10^{-5} to 2.39×10^{-5} m	0.06 cm^3	0.05 cm^3	0.07 cm^3
2.39×10^{-5} to 7.16×10^{-6} m	1.16 cm^3	0.93 cm^3	0.98 cm^3
7.16×10^{-6} to 3.58×10^{-6} m	0.03 cm^3	0.07 cm^3	0.08 cm^3
3.58×10^{-6} to 2.39×10^{-6} m	-	0.01 cm^3	0.04 cm^3
2.39×10^{-6} to 1.79×10^{-6} m	-	0 cm^3	0.01 cm^3
1.79×10^{-6} to 1.43×10^{-6} m	-	0 cm^3	-
less than 1.43×10^{-6} m	-	0.20 cm^3	-

Saturated hydraulic conductivity measurements were recently made on a 7.5 x 7.5 x 5 cm block of simulated ILAW glass[5]. The glass block was subjected to mechanical stress on all sides simultaneously to cause internal fracturing; approximately one to two fractures that progressed into the block were formed on each face. Care was taken to form at least some of the fractures to be connective, but none of the fractures to be connecting two opposite faces continuously. Overall, the fractures were conductive and randomly connected. The fractured blocks were secured together using a platinum wire wrap. The measured porosity of this block was 0.03, similar to the small cylinders discussed above and consistent with the expected ILAW glass porosity. Saturated hydraulic conductivity of the fractured glass block was measured using a static head permeameter method. Three replicates yielded an average value of 3.1×10^{-5} cm/s. This is significantly lower than the assumed value of Meyer and Serne (1999), but since this is a direct measurement on a fractured glass sample, it is given in Table 4.3 as the best-estimate value.

Table 4.3. Best-Estimate Parameter Values for ILAW Glass

ρ_p (g/cm^3)	ρ_b (g/cm^3)	θ_s	θ_r	α (cm^{-1})	n	K_s (cm/s)
2.68	2.63	0.02	0.0006	0.044	1.88	3.1×10^{-5}

[5] Saripalli, K.P., M.J. Lindberg and P.D. Meyer. 2003. Effect of Chemical Reactions on the Hydraulic Properties of ILAW Near-field Materials: Experimental Investigation, Letter Report to CH2MHill Hanford Group, Inc., September 30, 2003, Pacific Northwest National Laboratory, Richland Washington.

Figure 4.1. Photograph of Fractured Glass Cylinder 2 Inches in Diameter and 2.75 Inches High

4.4.2 LLW/MLLW

As stated previously, there are generally no performance requirements for the waste form or the waste package for most LLW (Mann et al. 2003a). For MLLW, waste package and waste form performance is generally provided by concrete containers or by grouting the waste. In past PAs (Wood 1995,1996), relatively simple, conservative models of waste form release have been used. These simple models do not require the unsaturated hydraulic properties of the LLW/MLLW waste forms. Should flow and transport through the LLW/MLLW packages be explicitly modeled, however, the concrete properties from Meyer and Serne (1999) can be used to represent the grout/concrete components of the waste packages. These parameters were obtained using centrifuge measurements on 50-year-old concrete cores taken from a bunker on the Hanford Site and are presented below.

Table 4.4. Best-Estimate Parameter Values for Concrete

ρ_p (g/cm^3)	ρ_b (g/cm^3)	θ_s	θ_r	α (cm^{-1})	n	K_s (cm/s)
2.63	2.46	0.067	0.00	3.87×10^{-5}	1.29	1.33×10^{-9}

4.4.3 WTP Melters and Overpack

Should flow and transport through the WTP Melter waste packages be explicitly modeled, the residual waste material remaining in the WTP melters can be modeled as ILAW glass using the hydraulic parameters given in Table 4.3. Assuming the melters are grouted into their overpacks, the hydraulic parameters for concrete given in Table 4.4 can be used for the grouted portion of the waste package. The steel components of the melters and overpack will be impermeable as long as they are intact. Meyer and

Serne (1999) presented representative hydraulic parameters for fully corroded steel based on measurements made on crushed rock samples of hematite, goethite, and lepidocrocite, the expected dominant steel corrosion products. Those parameters are reproduced here for potential use in modeling the steel components of the WTP melter waste packages.

Table 4.5. Best-Estimate Parameter Values for Fully Corroded Steel

ρ_p (g/cm^3)	ρ_b (g/cm^3)	θ_s	θ_r	α (cm^{-1})	n	K_s (cm/s)
4.16	2.30	0.39	0.04	0.0008	1.77	2.2×10^{-6}

4.4.4 Supplemental ILAW Waste Forms

As discussed previously, it is assumed for the IDF PA that all WTP supplemental technology waste is processed by bulk vitrification (Puigh 2004). Based on current tests of this process (see Section 2.2.4.4), the materials of the waste package may include the steel container, insulating foam board, sand, an insulating cast (brick-like) material, and the glass waste vitrification product. Parameters for fully corroded steel were given in Section 4.4.3. No properties are provided here for the foam board. Properties of backfill (Section 4.5) can be used for the sand. (If the sand used has a more uniform particle size distribution than the backfill, these parameters should be modified.) Until more specific data becomes available, the vitrified waste product can be assigned the parameters of the ILAW Glass given in Table 4.3.

Unsaturated hydraulic property measurements of cast materials are rare. Hall and Hoff (2002) discuss water flow in building materials, including brick materials, but do not report any water retention data. They provide a figure of water retention measurements on "common clay brick ceramic[6]" illustrating a van Genuchten model fit. This figure was scanned, the data were digitized, and Equation 3-2 was fit to the data. The resulting water retention parameters are given in Table 4.6. Physical properties were measured on a sample cast material being used in current bulk vitrification tests.[7] The particle and bulk densities are reported in Table 4.6. The particle density is outside the range of typical brick ceramic compositions (2.6 – 2.8 g/cm3) according to Hall and Hoff (2002). Total porosity calculated from these values is 0.27. Hall and Hoff (2002) cite various references reporting porosity measurements ranging from approximately 0.1 to 0.45 depending on the type of brick material. Corresponding bulk densities range from about 2.4 – 1.5 g/cm^3 with an estimated average particle density of 2.68 g/cm^3. Effective porosity measured on the sample cast material was reported to be 0.17[8], only 63% of the total porosity. Should further investigation of this value result in its being raised, this would not change the estimates of the other water retention parameters. Saturated water content is less than the effective porosity because the wetting curve data

[6] Hall and Hoff (2002), Figure 2.3, page 50.

[7] E.M. Pierce, May 2004, personal communication.

[8] E.M. Pierce, May 2004, personal communication.

(from Figure 2.3 of Hall and Hoff) were used to estimate the water retention parameters. (The data of Hall and Hoff exhibited significant hysteresis.) Due to the heat associated with the vitrification process, this material is likely to be dry when moved to the IDF. Use of the wetting curve was therefore felt to be appropriate.

Hall and Hoff (2002) reference two measurements of the hydraulic conductivity in clay brick ceramic. The values reported are 3.2×10^{-6} cm/s for a brick with porosity of 0.40 and 3.8×10^{-7} cm/s for a brick with porosity of 0.31. The geometric mean of these values is included in Table 4.6.

Table 4.6. Best-Estimate Parameter Values for the Cast Material of the Bulk Vitrification Waste Package

ρ_p (g/cm^3)	ρ_b (g/cm^3)	θ_s	θ_r	α (cm^{-1})	n	K_s (cm/s)
3.1	2.26	0.15	0.00	0.00064	1.90	1.1×10^{-6}

4.5 Backfill

The best-estimate parameters for the backfill presented in Meyer and Serne (1999) were based on analysis of a single sample composited from 85 individual samples obtained at depths of 3 to 17 m from 200 East Area boreholes. Additional data has since been collected and is used to update the backfill hydraulic parameter estimates.

Two samples were collected from a borehole (B8501 discussed in Reidel et al. 1998) adjacent to borehole 299-E17-21 near the southwest corner of the IDF site. The samples were collected at depths of 6.7 and 8.2 m and texturally were classified as sands. Water retention measurements were made on these samples using the method of Lenhard and Parker (1988). Bulk density for these measurements was 1.65 g/cm^3. Unsaturated hydraulic conductivity measurements were conducted on the same samples using the steady-state centrifugation method (ASTM D6527-00). Bulk densities for the samples analyzed in the centrifuge were higher at approximately 1.86 g/cm^3. In addition to these two samples, 60 samples were collected at depths of 4 to 16 m from an experimental site adjacent to the IDF site (the Vadose Zone Transport Field Study Site). These samples were collected in a (mostly) undisturbed condition and analyzed for particle size distribution, bulk density, water retention, and hydraulic conductivity (Schaap et al. 2003). For these 60 samples, sand percentage was always greater than 72.5 percent, clay percentage was always less than 7.5 percent and silt percentage ranged from 6 to 22 percent. Bulk densities ranged from 1.39 to 1.71 g/cm^3 with an average value of 1.57 g/cm^3.

Excavation spoils and borrow material from the IDF site are likely to be used in two conditions: a relatively high bulk density application in which the soil is able to be well compacted, and a relatively low bulk density application in which compaction will be more difficult (such as when the soil is used to fill between the waste packages). The data from the samples described above were divided into two groups based on the sample bulk densities with a density of 1.60 g/cm^3 being the cutoff between the groups. Estimated parameter values were then examined to determine best-estimate values for the IDF backfill materials for each of the two groups. The direct water retention and saturated hydraulic

conductivity measurements were used for the data from Schaap et al. (2003). A particle density of 2.71 g/cm^3 was assumed. Values for α, n and K_s are based on the geometric means of the measurements.

Table 4.7. Best-Estimate Parameter Values for Low- and High-Density Backfill

ρ_p (g/cm^3)	ρ_b (g/cm^3)	θ_s	θ_r	α (cm^{-1})	n	K_s (cm/s)
2.71	1.51	0.37	0.03	0.057	2.8	1.86×10^{-2}
2.71	1.66	0.35	0.03	0.065	1.7	4.91×10^{-3}

4.6 Summary Tables

Values of best-estimate parameters for near-field materials of the IDF are summarized here in two tables: one for the materials of the surface cover and one for the remainder of the materials. For those materials not appearing in tables earlier in this chapter, values were taken from Meyer and Serne (1999) and are presented here solely for the convenience of the reader.

Table 4.8. Summary of Best-Estimate Parameter Values for Components of the Surface Cover

Material	ρ_p (g/cm^3)	ρ_b (g/cm^3)	θ_s	θ_r	α (cm^{-1})	n	K_s (cm/s)
Silt Loam-Gravel Admix	2.72	1.48	0.456	0.0045	0.0163	1.37	8.4 x 10-5
Compacted Silt Loam	2.72	1.58	0.39	0.09	0.006[9]	1.92	5.2×10^{-5}
Sand Filter	2.76	1.88	0.318	0.030	0.538	1.68	8.58 x 10-5
Gravel Filter	2.72	1.94	0.290	0.026	8.10	1.78	1.39 x 10-2
Gravel Drainage	2.72	1.94	0.290	0.006	17.8	4.84	2.0
Asphaltic Concrete	2.63	2.52	0.04	0.000	1.0 x 10-7	2.0	1.0 x 10-11

[9] Drainage curve α. Imbibition curve α is 0.014 cm^{-1}.

Table 4.9. Summary Table of Best-Estimate Parameter Values for IDF Materials

Material	ρ_p (g/cm^3)	ρ_b (g/cm^3)	θ_s	θ_r	α (cm^{-1})	n	K_s (cm/s)
ILAW Glass	2.68	2.63	0.02	0.0006	0.044	1.88	3.1×10^{-5}
Concrete	2.63	2.46	0.067	0.00	3.87×10^{-5}	1.29	1.33×10^{-9}
Fully Corroded Steel	4.16	2.30	0.39	0.04	0.0008	1.77	2.2×10^{-6}
Bulk Vit. Cast Material	3.1	2.26	0.15	0.00	0.00064	1.90	1.1×10^{-6}
Low Density Backfill	2.71	1.51	0.37	0.03	0.057	2.8	1.86×10^{-2}
High Density Backfill	2.71	1.66	0.35	0.03	0.065	1.7	4.91×10^{-3}

5.0 Best-Estimate Values for Transport Parameters of Near-Field Materials

Meyer and Serne (1999) discussed the best-estimate transport parameter values for near-field materials of the ILAW disposal facility. Consideration of transport parameters was limited to dispersivity and diffusion coefficients. Diffusion is expected to be the dominant transport mechanism from the IDF. Parameters governing the chemistry of the near-field materials (e.g., adsorption distribution coefficients and solid phase solubility controls) can be found in other data packages (Pierce et al. 2004; Krupka et al. 2004).

5.1 Dispersivity

Meyer and Serne (1999) recommended a dispersivity value of 10 cm based on a field experiment conducted at the IDF site[10], and the expected conditions of the IDF near field (limited scale, relative homogeneity, low pore water velocities). No modification of this value is recommended here.

5.2 Diffusion Coefficient

5.2.1 Concrete

Diffusion in concrete was reviewed in detail by Meyer and Serne (1999) with best-estimate apparent diffusion coefficient values for a variety of constituents provided. That discussion is not repeated here and no modification of the best-estimate diffusion coefficient values is recommended.

5.2.2 Backfill (and Other Granular Materials)

Measurements of intrinsic diffusion coefficients were reported in Conca and Wright (1990, 1991) for a variety of materials, including sediments from the Hanford Site. Conca and Wright (1991) observed that the measured $D_i(\theta)$ relationship (for a chemically nonreactive solute) was remarkably similar for a variety of materials, which included porous and nonporous tuff gravels, bentonite clays, Hanford sandy soils and gravels, and whole rock cores of non-welded tuff. Conca and Wright (1990) also observed, however, that the diffusion coefficient at a given water content tended to be lower for samples with larger particle sizes and more hydrophobic mineral surfaces.

The data of Conca and Wright (1991) were fit to the power function model given earlier as Equation 3-6 [$D_i(\theta) = a\, D_f\, \theta^b$].Using a value of $D_f = 1.84 \times 10^{-5}$ cm^2/s resulted in best-fit values for the coefficients

[10] Ward, A.L., R.E. Clayton and J.S. Ritter. 1998. Hanford Low-Activity Tank Waste Performance Assessment Activity: Determination of In Situ Hydraulic Parameters of the Upper Hanford Formation. Letter Report to Fluor Daniel Hanford, Inc., December 31, 1998, Pacific Northwest National Laboratory, Richland, Washington.

of a = 1.65 and b = 1.96. The data of Conca and Wright (1991) are shown in Figure 5.1 as the circles, with the fitted relationship represented by the dashed curve.

The intrinsic diffusion coefficient was estimated for two sand samples obtained from a borehole near the southwest corner of the IDF site and for two coarse sand samples obtained northeast of the IDF site at the former grout site using electrical conductivity measurements made at a series of water content values following the procedure described in Conca and Wright (1990). The estimated diffusion coefficients for the grout site sand and IDF borehole sands are shown on Figure 5.1(as the solid symbols). The borehole sand data lies very close to the data of Conca and Wright (1991) although the minimum water contents were 8 – 10%, much larger than the minimum values measured by Conca and Wright (1991). (Measurements using the centrifuge equipment were limited to hydraulic conductivities greater than about 5×10^{-10} cm/s.) The grout site samples had diffusion coefficients that were somewhat smaller than the range of values measured by Conca and Wright (1991), particularly at the lowest water content value measured for each sample. The smaller diffusion coefficients for this relatively coarse material are consistent with the observations of Conca and Wright (1990).

A linear fit to the logarithm of the combined diffusion data for the grout site and borehole sand samples resulted in best-fit values for the parameters of the power function of a = 3.95, b = 2.64. The estimated variance of these parameter values was much larger than for the fit to Conca and Wright's data. The best-fit parameter values for the complete set of data were a = 1.49, b = 1.96. A value of $D_f = 1.84 \times 10^{-5}$ cm^2/s was assumed in determining the empirical parameters. These best-fit power function relationships are included in Figure 5.1.

It is recommended that Equation 3-6 be used in the ILAW PA simulations to model diffusion in backfill and other granular materials of the near field. The results presented here suggest that a = 1.49, b = 1.96 are appropriate parameters for this diffusion model. The free-water diffusion coefficients, D_f, for individual contaminants can be selected from Table 5.3 of Meyer and Serne (1999) or calculated using one of the available equations (see Grathwohl, 1998).

5.2.3 ILAW Glass

Measurements of diffusion of three solutes (Cs, Sr, and PFBA) through a saturated fractured glass block were recently made on a 7.5 x 7.5 x 5 cm block of simulated ILAW glass (LAWBP1)[11]. The glass block was subjected to mechanical stress on all sides simultaneously to cause internal fracturing; approximately one to two fractures that progressed into the block were formed on each face. Care was taken to form at least some of the fractures to be connective, but none of the fractures to be connecting two opposite faces continuously. Overall, the fractures were conductive and randomly connected. The

[11] Saripalli, K.P., M.J. Lindberg and P.D. Meyer. 2003. Effect of Chemical Reactions on the Hydraulic Properties of ILAW Near-field Materials: Experimental Investigation, Letter Report to CH2MHill Hanford Group, Inc., September 30, 2003, Pacific Northwest National Laboratory, Richland Washington.

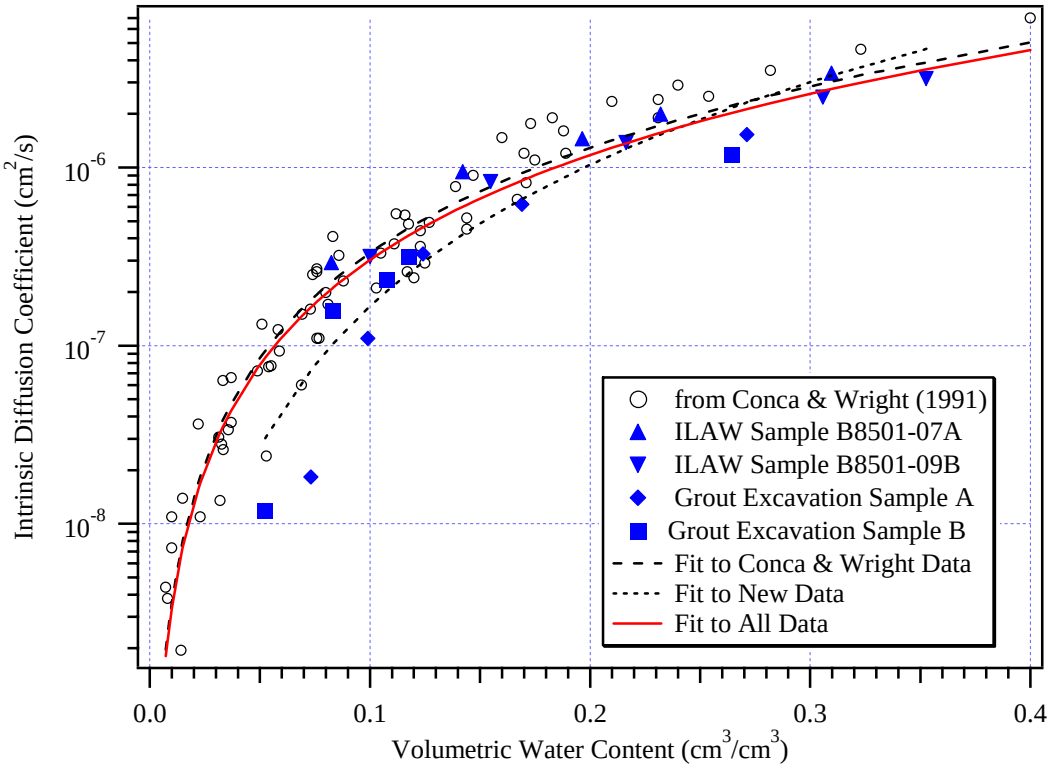

Figure 5.1. Diffusion Coefficient Estimates from Conca and Wright (1991) and for samples obtained near the IDF Site. Best-fit power function relationships (Equation 3-6) are shown as well.

fractured blocks were secured together using a platinum wire wrap. Diffusion experiments were conducted using an experimental method similar in design to that reported by Grathwohl (1998) called the time-lag method. In this method, a constant concentration boundary condition is maintained at the inlet face of the porous medium over a long period of time (typically several weeks depending on the D_i of the particular solute and medium combination). The mass of solute at the outlet face is monitored as a function of time to yield a solute mass – time relationship that can be used to obtain the diffusion coefficient. Under saturated conditions, the diffusions coefficients obtained from the Cs, Sr, and PFBA tracers were 1.42×10^{-5}, 1.66×10^{-5}, and 1.54×10^{-5} cm2/s, respectively, in a fractured glass block with a porosity of 0.016. These results suggest that the assumption of diffusion coefficients on the order of 10^{-5} cm^2/s for saturated ILAW fractured glass media appears to be reasonable.

The relationship for the intrinsic diffusion coefficient as a function of water content recommended in the previous section for backfill and other granular materials and expressed in Figure 5.1 is inappropriate for low-porosity, fractured glass waste. Since the ILAW glass is expected to have a porosity of just a few percent (best-estimate saturated water content is two percent), application of this relationship will result in very small diffusion coefficient values within the glass waste even under saturated conditions. This contradicts the laboratory measurements discussed above. If we assume that the intrinsic diffusion coefficient in the glass waste is a very low value (e.g., 10^{-7} cm^2/s) at the residual water content (0.0006 cm^3/cm^3) and that the free-water diffusion coefficients are on the order of 1.5×10^{-5} cm^2/s at saturation,

then diffusion within the glass waste will be extremely sensitive to water content within the glass. Since the actual water content within the glass is uncertain, we recommend choosing a constant, conservative value for the intrinsic diffusion coefficient in the ILAW glass. For example, the use of Equation 3-6 with parameters a = 1, b = 0 will maximize diffusion within the glass waste. The effect of this assumption can be examined in the sensitivity analyses conducted for the IDF PA.

5.2.4 Supplemental ILAW Waste Forms

Diffusion in the bulk vitrification glass waste material can be modeled in the same manner as the ILAW glass. For the cast (brick-like) insulating material present in the bulk vitrification waste package, it is recommended that diffusion be modeled using the power function (Equation 3-6) as discussed in Section 3.9. Buchwald (2000) measured diffusion in a brick sample as a function of water content using methods similar to those of Conca and Wright (1990). They fit a power function model (Equation 3-6) to their results, finding best-fit empirical parameters of a = 1.9, b = 1.6. Their brick material had a bulk density of 1.81 g/cm^3, particle density of 2.81 g/cm^3, total porosity of 0.36, and an effective porosity of 0.34.

6.0 Issues Affecting Parameter Values

6.1 Changes in Parameter Values Over Time

A number of the near-field materials may undergo significant changes over time, potentially affecting the performance of the IDF disposal facility. These changes will be caused by natural processes and in response to chemical changes in the near-field environment resulting from degradation of the waste forms. The materials for which hydraulic property changes over time are expected to most significantly impact the transport of contaminants are the surface cover materials, the steel and concrete overpacks, and the waste forms themselves. In addition, changes in backfill material are potentially important.

Changes in recharge through the surface cover either as a result of subsidence or in response to expansion of the waste containers due to steel corrosion are not discussed here. While these processes will not produce changes in the small-scale hydraulic properties of the surface cover materials (with the exception of the low-permeability asphaltic concrete layer), they may significantly affect the overall performance of the cover. Potential variations in the recharge rate over time are discussed in the recharge data package (Fayer and Szecsody 2004).

Steel will corrode over time and concrete will gradually degrade. Meyer and Serne (1999) provided unsaturated hydraulic parameter values for fully corroded steel and completely degraded concrete. They recommended sensitivity simulations to examine the impact of the change in these material properties on the performance of the facility. With the potential addition of significant amounts of steel in the form of the WTP melter overpacks, the issue of volume expansion during steel corrosion should be revisited.

Of the expected waste forms in the IDF, the ILAW glass has been the most extensively studied to develop models of its corrosion over time and consequent release of contaminants. In laboratory experiments the glass matrix has been shown to exhibit a propensity for dissolution and secondary mineral precipitation (McGrail et al., 2000). The resulting aqueous environment in the trench is marked by significant excursions in many of the physico-chemical parameters that influence its geochemistry, such as pH, ionic strength and solution composition. In controlled laboratory experiments, McGrail et al. (2000) established that the concentrations of Si, Na, K and Al register such dramatic excursions and obtained evidence of significant precipitation of secondary mineral phases. Precipitation of such minerals can cause a significant reduction in porosity and permeability by plugging pore throats of porous materials. Changes in these two basic properties of the medium also result in significant changes in the related properties (i.e., relative permeability, fluid-fluid and fluid-solid interfacial areas, and pore and particle size distributions) and the constitutive relationships among these properties (Saripalli et al. 2001). This fact, coupled with the very long time frames of interest (thousands of years) during which temporal changes in the near-field hydrology and geochemistry are to be expected, suggests that such changes may impact IDF performance.

Experiments and modeling research have been conducted to quantitatively characterize the hydraulic properties of representative ILAW glass media and the effect of physico-chemical reactions (especially secondary mineral precipitation) on these properties. In this context, it should be noted that the ILAW glass is expected to progressively fracture due to the combined effects of mechanical fracturing and glass

corrosion reactions. Such disintegration is likely to reduce the initial glass monolith into increasingly fractured, rubbelized and granular material, over many years. As such, the experimental and modeling investigations were designed to evaluate the effect of chemical reactions on the hydraulic properties of single-fracture, rubbelized and granular ILAW glass media. Results from these experiments and modeling indicated that the hydrologic properties of ILAW and the surrounding backfill can change significantly due to glass corrosion reactions (Freedman et al. 2003, 2004).

Mechanically fractured glass blocks, prepared as discussed in Section 4.4.1, were subjected to accelerated corrosion using a modified Vapor Hydration Test (VHT) procedure[12]. A reduction in porosity ranging from 33 to 51 percent was measured in three blocks (one of HAN-28 glass and two of LAWBP1 glass) due to a reaction precipitate deposited as a layered film on the glass surfaces. Measured saturated hydraulic conductivity also decreased in general as a result of the VHT reaction. The observed decrease ranged from none to almost an order of magnitude. In general the effect of the reaction on the saturated hydraulic conductivity was more significant for the HAN-28 glass (the more reactive glass).

A critical component of reactive transport modeling to determine the suitability of disposing of ILAW glass is the identification of key mineral assemblages affecting the porosity and permeability of both the glass and near- and far-field materials. In Freedman et al. (2003), two different classes of geochemical models were used to identify mineral precipitation and dissolution potentials for the disposal of ILAW. The first was a static geochemical model that did not consider the effects of transport. The second model was dynamic, and combined geochemical reactions with hydrogeological processes such as advection, diffusion and dispersion. This reactive transport model also included an innovative application of a depositional film model for determining changes in permeability due to mineral precipitation and dissolution reactions. Although both models described solid-aqueous phase reactions kinetically, the two models identified two different sets of mineral assemblages affecting the porosity and permeability of the media. These markedly different results were due to transport considerations, the most significant of which were the spatial variability in aqueous concentrations, and advection and diffusion of dissolved glass constituents into the backfill materials. This work showed that, for the prediction of geochemical behavior of engineered system, such as the IDF disposal facility, the traditional reaction path modeling approach using static (batch) models alone was not sufficient for an accurate assessment of the precipitation of key mineral assemblages and their effect on the geochemical and hydraulic behavior of the geomedia. Reactive transport modeling improved this assessment significantly. The static model was useful in identifying potential minerals to be included in the reactive transport simulations. The dynamic model, however, ultimately determined the key mineral assemblages affecting both the geochemical behavior and the hydraulic properties of the geomedia in the presence of a flowing aqueous phase.

In Freedman et al. (2004), a film depositional modeling approach was developed for modeling changes in permeability due to mineral precipitation and dissolution reactions in unsaturated porous

---

[12] Saripalli, K.P., M.J. Lindberg, J.V. Crum, M.J. Schweiger, and P.D. Meyer. 2002. Effect of Chemical Reactions on the Hydraulic Properties of ILAW Near-field Materials: Experimental Investigation, Letter Report to CH2MHill Hanford Group, Inc., September 30, 2002, Pacific Northwest National Laboratory, Richland Washington.

media. This model is appropriate for describing ILAW glass dissolution and secondary mineral precipitation in the IDF. The model is based on the assumption that the mineral precipitate is deposited on the pore walls as a continuous film, which may cause a reduction in permeability. Previous work in saturated media has used continuous pore-size distributions to represent the pore space. In Freedman et al. (2004), the film depositional model was developed for a discrete pore-size distribution, which was determined using the unsaturated hydraulic properties of the porous medium. This facilitated the process of dynamically updating the unsaturated hydraulic parameters used to describe fluid flow through the media. Single mineral test simulations were conducted to test both the Mualem (1976) and Childs and Collis-George (1950) permeability models. Results from simulation of the simultaneous dissolution of ILAW glass and secondary mineral precipitation showed that the film depositional models yielded physically reasonable predictions of permeability changes due to solid-aqueous phase reactions. The film depositional model has been implemented in STORM (Bacon et al. 2000), which is the model used in the ILAW PA simulations and which will be used in the 2005 IDF PA simulations.

6.2 Uncertainty Assessment

Meyer and Serne (1999) discussed uncertainty in parameter values and provided recommendations for upper and lower bounds on hydraulic parameters for a number of near-field materials. These bounding values were not used in the 2001 ILAW PA (Mann et al. 2001), however, and are therefore not updated here. The approach to uncertainty assessment that was taken in the previous ILAW PA's has been to identify a small number of sensitivity cases for which simulations are conducted to identify the impact of individual parameters or processes on the facility performance. The assessment of uncertainty in complex modeling is an active area of research. An example of such an assessment for a waste disposal application comparable to the IDF is the uncertainty assessment conducted for the Waste Isolation Pilot Plant (WIPP) (Helton et al. 2000 and related papers). Even if the sensitivity of model results to parameter values is the only interest, there are a number of systematic methods that can be used to explore model sensitivities in a comprehensive manner (Saltelli et al. 2000, 2004). Some of these methods are designed for application to complex models that require significant computational time for a single run, such as the IDF PA models. Campolongo et al. (2000) provide a summary of such screening methods.

6.3 Upscaling and Equivalent Parameter Values

Wood (2000) provides a review of upscaling methods for describing unsaturated flow emphasizing the potential needs of the near-field IDF environment. He groups the methods that can be used to upscale unsaturated flow properties into the following categories: (1) stochastic (regular perturbation) methods, (2) renormalization theory, and (3) volume averaging/homogenization methods and provides a brief review of each. In addition he includes a non-upscaling method referred to as: (4) full-resolution numerical modeling. For practical applications, the most reasonable approach is probably one that uses *any* upscaling technique (provided that the constraints for their validity are met) for upscaling in regions where the variations of the parameter fields are small. For upscaling in regions where the structure is more complex, such as in the IDF near-field environment, only the homogenization and volume averaging approaches are probably suitable. Previous ILAW PA simulations have not relied on upscaled properties in the near-field environment, but have attempted to use full-resolution numerical modeling to the limit of the available computational capabilities. Improvements in codes (such as the parallel computation

capabilities added to the STORM model) continue to enhance the ability to represent the geometry of the contrasting materials within the near field (e.g., backfill sand adjacent to glass waste) while including the desired complex reactions of waste form degradation.

7.0 Conclusions

This report has discussed issues related to the appropriate hydraulic and transport parameters to use in simulations of the IDF disposal facility for the 2005 IDF PA. This report is limited to those materials, both natural and man-made, that will be used within the near-field environment of the IDF disposal facility. Values for physical, hydraulic, and physical transport parameters are provided for those parameters that have been updated from the values presented in Meyer and Serne (1999), the data package for the 2001 ILAW PA. The report also includes a discussion of changes in material properties over time and how these changes are expected to affect the parameter values. Brief discussions of uncertainty assessment and upscaling in the near-field environment are included.

The parameter values provided in this report provide a starting point for the PA simulations. Changes in facility design, additional information and data that may become available, and unanticipated considerations may require that these parameter values be altered in the PA simulations. If this occurs, the new parameter values should be justified and the issues related to uncertainty and changes over time should be addressed for the new parameter values. Related parameters may also be used in other data packages being assembled for the 2005 IDF PA. These data packages have not all been reviewed for consistency with this report.

8.0 References

Arya, L.M. and J.F. Paris. 1981. "A Physicoempirical Model to Predict the Soil Moisture Characteristic from Particle-Size Distribution and Bulk Density Data," *Soil Sci. Soc. Am. J*., 45:1023-1030.

Arya L.M., F.J. Leij, and M.T. van Genuchten. 1999a. "Scaling Parameter to Predict the Soil Water Characteristic from Particle-Size Distribution Data," *Soil Sci. Soc. Am. J*., 63 (3):510-519.

Arya L.M., F.J. Leij, P.J. Shouse. 1999b. "Relationship between the Hydraulic Conductivity Function and the Particle-Size Distribution," *Soil Sci. Soc. Am. J*., 63(5):1063-1070.

ASTM D6527-00. Standard Test Method for Determining Unsaturated and Saturated Hydraulic Conductivity in Porous Media by Steady-State Centrifugation, American Society of Testing and Materials, Philadelphia, Pennsylvania.

Bacon, D., M.D. White, and B.P. McGrail. 2000. *Subsurface Transport Over Reactive Multiphases (STORM): A General, Coupled, Nonisothermal Multiphase Flow, Reactive Transport, and Porous Medium Alteration Simulator, Version 2, User's Guide*, PNNL-13108, Pacific Northwest National Laboratory, Richland, Washington.

Bouwer, H. and R.C. Rice. 1983. "Effect of stones on hydraulic properties of vadose zones," in *Proceedings of the characterization and monitoring of the vadose (unsaturated) zone,* National Water Well Association, Worthington, Ohio.

Buchwald, A. 2000. "Determination of the ion diffusion coefficient in moisture and salt loaded masonry materials by impedance spectroscopy," in *3rd Int. PhD Symposium*, Oct. 11-13, 2000, Vienna, Vol. 2, pp. 475-482.

Burbank, D.A. 2002. *Preliminary Closure Plan for the Immobilized Low-Activity Waste Disposal Facility Project*, RPP-69111, Revision 1, CH2MHILL Hanford Group, Inc., Richland, Washington.

Campbell, G.S. 1985. "Soil Physics with BASIC," In *Developments in Soil Science 14*, Elsevier Science Publishers B.V., New York, New York.

Campolongo, F., J. Kleinen, and T. Andres. 2000. "Screening Methods," in *Sensitivity Analysis,* A. Saltelli, K. Chan, and E.M. Scott (eds.), John Wiley & Sons, Ltd., West Sussex, England.

Cedergren, H.R. 1989. *Seepage, Drainage, and Flow Nets*, Third Edition. John Wiley and Sons, Inc., New York, New York.

CHG. 2003a. *Integrated Mission Accelerated Plan*, RPP-13678, CH2M HILL Hanford Group, Inc., Richland, Washington.

CHG. 2003b. *Integrated Disposal Facility (IDF) Phase I Critical Systems Design Report*, RPP-18486, CH2M HILL Hanford Group, Inc., Richland, Washington.

CHG. 2003c. *Integrated Disposal Facility (IDF) Detailed Design: Specifications* (DOE/CHG Review Draft, December 2003), RPP-18489, CH2M HILL Hanford Group, Inc., Richland, Washington.

Childs, E.C. and N. Collis-George. 1950. "The permeability of porous materials," *Proc. Roy. Soc. London A*, 201:392-405.

Conca, J.L. and J.V. Wright. 1990. "Diffusion coefficients in gravel under unsaturated conditions," *Wat. Resour. Res.*, 26(5):1055-1066.

Conca, J.L. and J.V. Wright. 1991. "Aqueous diffusion coefficients in unsaturated materials," *Mat. Res. Soc. Symp. Proc.*, Vol. 212, pp. 879-884.

Dane, J.H. and G.C. Topp (eds.). 2002. *Methods of Soil Analysis: Part 4 - Physical Methods*, Soil Science Society of America, Madison, Wisconsin.

Dane, J.H. and J.W. Hopmans. 2002. "Pressure Cell," in *Methods of Soil Analysis: Part 4 - Physical Methods*, J.H. Dane and G.C. Topp (eds.), Soil Science Society of America, Madison, Wisconsin.

DOE. 1993a. *Focused Feasibility Study of Engineered Barriers for Waste Management Units in the 200 Areas*, DOE/RL-93-33, Rev. 1, U.S. Department of Energy, Richland Operations Office, Richland, Washington.

DOE. 1993b. *Hanford Site Solid Waste Landfill Permit Application*, DOE/RL-90-38, Rev. 1, U.S. Dept. of Energy, Richland, Washington

DOE. 2004. *Final Hanford Site Solid (Radioactive and Hazardous) Waste Program Environmental Impact Statement Richland, Washington*, DOE/EIS-0286F, U.S. Department of Energy Richland Operations Office, Richland, Washington.

Ecology. 1987. *Solid Waste Landfill Design Manual*, No. 87-13, Parametrix, Inc., Bellevue, WA, for Washington State Department of Ecology, Olympia, Washington.

Environmental Protection Agency (EPA). 1989. *Technical Guidance Document: Final Covers on Hazardous Waste Landfills and Surface Impoundments*, EPA 530-SW-89-047, U.S. Environmental Protection Agency, Washington, D. C.

Fayer, M.J. and T.B. Walters. 1995. *Estimated Recharge Rates at the Hanford Site*, PNL-10285, Pacific Northwest Laboratory, Richland, Washington.

Fayer, M.J. and C.S. Simmons. 1995. "Modified soil water retention functions for all matric suctions," *Wat. Resour. Res.*, 31(5)1233-1238.

Fayer, M.J., E.M. Murphy, J.L. Downs, F.O. Khan, C.W. Lindenmeier, and B.N. Bjornstad. 1999. *Recharge Data Package for the Immobilized Low-Activity Waste 2001 Performance Assessment,* PNNL-13033, Pacific Northwest National Laboratory, Richland, Washington.

Fayer, M.J. and J.E. Szecsody. 2004. *Recharge Data Package for the Integrated Disposal Facility 2005 Performance Assessment,* PNNL-XXXXX, Pacific Northwest National Laboratory, Richland, Washington.

Flint, A.L. and L.E. Flint. 2002a. "Particle Density," in *Methods of Soil Analysis: Part 4 - Physical Methods*, J.H. Dane and G.C. Topp (eds.), Soil Science Society of America, Madison, Wisconsin.

Flint, A.L. and L.E. Flint. 2002b. "Porosity," in *Methods of Soil Analysis: Part 4 - Physical Methods*, J.H. Dane and G.C. Topp (eds.), Soil Science Society of America, Madison, Wisconsin.

Flury, M. and T.F. Gimmi. 2002. "Solute Diffusion," in *Methods of Soil Analysis: Part 4 - Physical Methods*, J.H. Dane and G.C. Topp (eds.), Soil Science Society of America, Madison, Wisconsin.

Freedman, V.L., D.H. Bacon, K.P. Saripalli, and P.D. Meyer. 2004. "A film depositional model of permeability for mineral reactions in unsaturated media," *Vadose Zone Journal* (in press).

Freedman, V.L., K.P. Saripalli, and P.D. Meyer. 2003. "Influence of mineral precipitation and dissolution on hydrologic properties of porous media in static and dynamic systems," *Applied Geochemistry*, 18:589-606.

Gee, G.W. and D. Or. 2002. "Particle Size Analysis," in *Methods of Soil Analysis: Part 4 - Physical Methods*, J.H. Dane and G.C. Topp (eds.), Soil Science Society of America, Madison, Wisconsin.

Grathwohl, P. 1998. *Diffusion in Natural Porous Media: Contaminant Transport, Sorption/Desorption and Dissolution Kinetics,* Kluwer Academic Publishers, Boston, Massachusetts.

Grossman, R.B. and T.G. Reinsch. 2002. "Bulk Density and Linear Extensibility," in *Methods of Soil Analysis: Part 4 - Physical Methods*, J.H. Dane and G.C. Topp (eds.), Soil Science Society of America, Madison, Wisconsin.

Hajek, B.F. 1966. *Soil Survey Hanford Project in Benton County Washington*, BNWL-243, Pacific Northwest Laboratory, Richland, Washington.

Hall, C. and W.D. Hoff. 2002. *Water Transport in Brick, Stone, and Concrete,* Spon Press, New York, New York.

Helton, J.C., D.R. Anderson, G. Basabilvazo, H.-N. Jow, and M.G. Marietta. 2000. "Conceptual structure of the 1996 performance assessment for the Waste Isolation Pilot Plant," *Reliability Engineering and System Safety*, 69:151-165.

Hillel, D. 1980. *Applications of Soil Physics,* Academic Press, San Diego, California, 385 pp.

Hoitink D.J., K.W. Burk, J.V. Ramsdell, Jr., and W.J. Shaw. 2003. *Hanford Site Climatological Data Summary 2002 with Historical Data*, PNNL-14242, Pacific Northwest National Laboratory, Richland, WA.

Hopmans, J.W., J. Simunek, N. Romano, and W. Durner. 2002. "Inverse Methods," in *Methods of Soil Analysis: Part 4 - Physical Methods*, J.H. Dane and G.C. Topp (eds.), Soil Science Society of America, Madison, Wisconsin.

Kemper, W. D. 1986. "Solute Diffusivity." in *Methods of Soil Analysis, Part 1, Physical and Mineralogical Methods*, A. Klute (ed.), pp. 1007-1024, American Society of Agronomy, Madison, Wisconsin.

Kemper, W. D. and J.C. van Schaik. 1966. "Diffusion of salts in clay-water systems." *Soil Sci. Soc. Amer. Proc.*, 30:534-540.

Khaleel, R. 2004. *Far-Field Hydrology Data Package for Integrated Disposal Facility Performance Assessment*, RPP-20621, Rev. 0, CH2MHill Hanford Group, Richland, Washington.

Khaleel, R., J.F. Relyea, and J.L. Conca. 1995. "Evaluation of van Genuchten-Mualem relationships to estimate unsaturated hydraulic conductivity at low water contents." *Wat. Resour. Res.*, 31(11):2659-2668.

Khaleel, R., T.-C.J. Yeh, and Z. Lu. 2002. "Upscaled flow and transport properties for heterogeneous unsaturated media, *Wat. Resour. Res.*, 38 DOE:10.1029/2000WR000072.

Klute, A. 1986. "Water Retention: Laboratory Methods," in Methods of Soil Analysis: Part 1 - Physical and Mineralogical Methods, A. Klute (ed.), pp. 635-660, American Society of Agronomy, Madison, Wisconsin.

Krupka, K.P., D.I Kaplan, and R.J. Serne. 2004. *Geochemical Data Package for the 2005 Integrated Disposal Facility Performance Assessment*, PNNL-13037, Rev. 2, Pacific Northwest National Laboratory, Richland, Washington.

Lenhard, R.J. and J.C. Parker. 1987. "A model for hysteretic constitutive relations governing multiphase flow, 2. Permeability-saturation relations," *Wat. Resour. Res.*, 23(12):2197-2206.

Lenhard, R.J. and J.C. Parker. 1988. "Experimental validation of the theory of extending two-phase saturation-pressure relations to three-fluid phase systemss for monotonic drainage paths," *Wat. Resour. Res.*, 24(3):373-380.

Lenhard, R.J., J.C. Parker, and S. Mishra. 1989. "On the correspondence between Brooks-Corey and van Genuchten models," *ASCE J. Irrigation and Drainage Engineering*, 115(4):744-751.

Luckner, L., M.Th. van Genuchten, and D.R. Nielsen. 1991. "Reply," *Wat. Resour. Res.*, 27(4):663-664.

Mann, F.M. 2002. *Performance Objectives for the Hanford Immobilized Low-Activity Waste (ILAW) Performance Assessment*, RPP-13263, CH2M Hill Hanford Group, Inc., Richland, Washington.

Mann, F.M. 2003. *Annual Summary of the Integrated Disposal Facility Performance Assesment for 2003*, DOE/ORP-2000-19, Rev. 3, Office of River Protection, Department of Energy, Richland, Washington.

Mann, F.M. and R.J. Puigh. 2001. *Data Packages for the Hanford Immobilized Low-Activity Tank Waste Performance Assessment: 2001 Version*, HNF 5636, Rev. 2, prepared by Fluor Federal Services for Fluor Daniel Hanford Company, Richland, Washington.

Mann, F.M., K.C. Burgard, W.R. Root, R.J. Puigh, S.H. Finfrock, R. Khaleel, D.H. Bacon, E.J. Freeman, B.P. McGrail, S.K. Wurstner, and P.E. LaMont. 2001. *Hanford Immobilized Low-Activity Waste Performance Assessment: 2001 Version*, DOE/ORP-2000-24, Rev. 0, Office of River Protection, Department of Energy, Richland, Washington.

Mann, F.M, R.J. Puigh, S.H. Finfrock, R. Khaleel, and M.I. Wood. 2003a. *Integrated Disposal Facility Risk Assessment*, RPP-15834, CH2M Hill Hanford Group, Inc., Richland, Washington.

Mann, F.M., B.P. McGrail, D.H. Bacon, R.J. Serne, K.M. Krupka, R.J. Puigh, R. Khaleel, and S. Finfrock. 2003b. *Risk Assessment Supporting the Decision on the Initial Selection of Supplemental ILAW Technologies*, RPP-17675, Rev. 0, CH2M Hill Hanford Group, Inc., Richland, Washington.

McGrail, B.P., D.H. Bacon, J.P. Icenhower, W.L. Ebert, P.F. Martin, H.T. Schaef, and E.A. Rodgriguez. 2000. *Waste Form Release Data Package for the 2001 Immobilized Low-Activity Waste Performance Assessment*, PNNL Report 13043, Rev. 1., Pacific Northwest National Laboratory, Richland, Washington.

Meyer, P.D. and R.J. Serne. 1999. *Near Field Hydrology Data Package for the Immobilized Low-Activity Waste 2001 Performance Assessment*, PNNL-13035, Rev. 1, Pacific Northwest National Laboratory, Richland, Washington.

Millington, R.J. 1959. "Gas diffusion in porous media," *Science*, 130:100-102.

Mualem, Y. 1976. "A new model for predicting the hydraulic conductivity of unsaturated porous media," *Wat. Resour. Res*., 12(3):513-522.

Neitzel, D.A. (ed.). 1998. *Hanford Site National Environmental Policy Act (NEPA) Characterization*, PNNL-6415, Rev. 10, Pacific Northwest National Laboratory, Richland, Washington.

Nimmo, J.R. 1991. "Comment on the treatment of residual water content in 'A consistent set of parametric models for the two-phase flow of immiscible fluids in the subsurface' by L. Luckner et al." *Wat. Resour. Res.*, 27(4):661-662.

Papendick, R. I. and G. S. Campbell. 1980. “Theory and Measurement of Water Potential.” in *Water Potential Relations in Soil Microbiology,* Am. Soc. of Agron. Spec. Publication No. 9, Soil Science Society of America, Madison, Wisconsin, pp. 1-22.

Parker, J.C. and R.J. Lenhard. 1987. “A model for hysteretic constitutive relations governing multiphase flow, 1. Saturation-pressure relations,” *Wat. Resour. Res.*, 23(12):2187-2196.

Pierce, E.M., J.P. Icenhower, B.P. McGrail, B.P., and D.H. Bacon. 2004. *Waste Form Release Data Package for the 2005 Integrated Disposal Facility Performance Assessment*, PNNL-XXXX, Pacific Northwest National Laboratory, Richland, Washington.

Porter, L.K., W.D. Kemper, R.D. Jackson, and B.C. Stewart. 1960. “Chloride diffusion in soils as influenced by moisture content,” *Soil Sci. Soc. Am. Proc.*, 24:460-463.

Puigh, R. 2004. *Disposal Facility Data for the Hanford Integrated Disposal Facility Performance Assessment*, RPP-20691, CH2MHill Hanford Group, Inc., Richland, WA.

Reidel, S.P. 2004. *Geologic Data Package for 2005 Integrated Disposal Facility Waste Performance Assessment*, PNNL-14586, Pacific Northwest National Laboratory, Richland, Washington.

Reidel, S.P., K.D. Reynolds, and D.G. Horton. 1998. *Immobilized Low-Activity Waste Site Borehole 299-E17-21*, PNNL-11957, Pacific Northwest National Laboratory, Richland, Washington.

Romano, N., J.W. Hopmans, and J.H. Dane. 2002. “Suction Table,” in *Methods of Soil Analysis: Part 4 - Physical Methods*, J.H. Dane and G.C. Topp (eds.), Soil Science Society of America, Madison, Wisconsin.

Rossi, C. and J. R. Nimmo. 1994. “Modeling of soil water retention from saturation to oven dryness,” *Wat. Resour. Res.*, 30(3):701-708.

Saltelli, A., K. Chan, and E.M. Scott (eds.). 2000. *Sensitivity Analysis*, John Wiley & Sons, Ltd., Chichester, England.

Saltelli, A., S. Tarantola, F.Campolongo, and M. Ratto. 2004. *Sensitivity Analysis in Practice: A Guide to Assessing Scientific Models,* John Wiley & Sons, Ltd., Chichester, England, 232 pp.

Saripalli, K.P., P.D. Meyer, D.H. Bacon, and V.L. Freedman. 2001. “Changes in Hydrologic Properties of Aquifer Media due to Chemical Reactions: A Review,” *Critical Reviews in Environmental Science and Technology*, 31(4):311-349.

Schaap, M.J. and F.J. Leij. 2000. “Improved prediction of unsaturated hydraulic conductivity with the Mualem-van Genuchten model,” *Soil Sci. Soc. Am. J.*, 64:843-851.

Schaap, M. G., P. J. Shouse, and P. D. Meyer. 2003. *Laboratory Measurements of the Unsaturated Hydraulic Properties at the Vadose Zone Transport Field Study Site*, PNNL-14284, Pacific Northwest National Laboratory, Richland, Washington.

Stephens, D.B. and S. Heermann. 1988. “Dependence of anisotropy on saturation in a stratified sand,” *Wat. Resour. Res.*, 24:770-778.

van Genuchten, M.Th. 1980. “A closed-form equation for predicting the hydraulic conductivity of unsaturated soils,” *Soil Sci. Soc. Am. J.*, 44:892-898.

WDOT. 1991. “Specification for Road, Bridge, and Municipal Construction,” Washington Department of Transportation, Olympia, Washington.

Wood B.D. 2000. *Review of Upscaling Methods for Describing Unsaturated Flow*, PNNL-13325, Pacific Northwest National Laboratory, Richland, Washington.

Wood, M.I., R. Khaleel, P.D. Rittmann, A.H. Lu, S.H. Finfrock, R.J. Serne, and K.J. Cantrell. 1995. *Performance Assessment for the Disposal of Low-Level Waste in the 200 West Area Burial Grounds*, WHC-EP-0645, Westinghouse Hanford Company, Richland, Washington.

Wood, M.I., R. Khaleel, P.D. Rittmann, S.H. Finfrock, T.H. DeLorenzo, and D.Y. Garbrick. 1996. *Performance Assessment for the Disposal of Low-Level Waste in the 200 East Area Burial Grounds*, WHC-EP-0875, Westinghouse Hanford Company, Richland, Washington.

Zaslavsky, D. and G. Sinai. 1981. “Surface hydrology: IV. Flow in sloping layered soil,” *J. Hydraul. Div.*, Am. Soc. Civ. Eng., 107:1-93.

Zhang, Z.F., A.L. Ward, and G.W. Gee. 2003. “A tensorial connectivity-tortuosity concept to describe the unsaturated hydraulic properties of anisotropic soils,” *Vadose Zone Journal*, 2(3):313-321.

Distribution

No. of Copies

ONSITE

4 **CH2M Hill Group**

DC Comstock	H6-19
JG Field	H6-62
FM Mann	E6-35
G Parsons	H6-19

1 **U.S. Department of Energy/ORP**

PE LaMont	H6-60

2 **Fluor Daniel Hanford, Inc.**

BH Ford	E6-35
MI Wood	H8-44

2 **Fluor Government Group, Inc.**

R Khaleel	B4-43
RJ Puigh	B4-43

No. of Copies

31 **Pacific Northwest National Laboratory**

DH Bacon	K9-33
MP Bergeron	K9-33
RW Bryce	K6-75
JL Downs	K6-85
MJ Fayer	K9-33
VL Freedman	K6-36
MD Freshley	K9-33
GW Gee	K9-33
CT Kincaid	K9-33
K Krupka	K6-81
GV Last	K6-81
CW Lindenmeier	K6-81
BP McGrail	K6-81
PD Meyer (10)	BPO
L Morasch	K6-86
WE Nichols	K9-33
SP Reidel	K6-81
ML Rockhold	K9-33
KP Saripalli	K6-81
RJ Serne	K6-81
AL Ward	K9-33
F Zhang	K9-33